Comparison of the methylerythritol phosphate pathway and the isopentenol utilization pathway for astaxanthin production in *Escherichia coli*

by

Jared Harrison Roth

A thesis

presented to the University of Waterloo

in fulfillment of the

thesis requirement for the degree of

Master of Applied Science

in

Chemical Engineering

Waterloo, Ontario, Canada, 2020

Author's Declaration

I hereby declare that I am the sole author of this thesis. This is a true copy of the thesis, including any required final revisions, as accepted by my examiners.

I understand that my thesis may be made electronically available to the public.

Abstract

Astaxanthin is a red carotenoid belonging to the isoprenoid family of compounds. Currently, the most common method of producing astaxanthin is through chemical synthesis and natural production using *Haematococcus pluvialis*. However, there is an increased demand for natural pure astaxanthin, which can be achieved through heterologous production in *Escherichia coli*. To induce astaxanthin production, the genes *ggpps*, *crtB*, *crtI*, *crtY*, *cbfd* and *hbfd* were introduced into MG1655(DE3) *E. coli* in three constructs. The first used a plasmid system that constitutively expressed the genes up to β-carotene and contained two inducible operons for *cbfd* and *hbfd* expression (pAC-BETAipi/pCBFD1). The second system used a singular operon for all genes (p5T7-astaipi-ggpps), and the third contained two inducible operons and an extra copy of FPP synthase (*IspA*) (p5T7-lycipi-IspA/pACT7-astaipi). Each plasmid system was paired with either the wild-type methylerythritol phosphate (MEP) pathway of *E. coli*, an upregulated MEP pathway (trcMEP) or the isopentenol utilization pathway (IUP). Using the pAC-BETAipi/pCBFD1 system, astaxanthin production in Luria-Bertani (LB) media resulted in a moderate increase in total carotenoids with the overexpressed MEP pathway and the IUP pathway (2.7-fold over wild-type MEP for both). However, in M9 media, the strain expressing the IUP pathway improved production to 9.43 ± 2.21 mg/g dcw at 48 h, a 13.1-fold increase from the wild-type. The newly cloned plasmid systems had more modest results, yielding carotenoid contents of 3.58 ± 0.79 mg/g dcw (p5T7-astaipi-ggpps) and 3.53 ± 0.36 mg/g dcw (p5T7-lycipi-IspA/pACT7-astaipi) in M9 media. However, increasing the inducer concentration from 0.1 mM to 0.7 mM in the p5T7-astaipi-ggpps strain resulted in similar titres compared to the pAC-BETAipi/pCBFD1 system, suggesting that enzyme expression was poorly balanced in the single plasmid system. HPLC analysis determined the highest astaxanthin purity to be 63.08 ± 0.36% in the p5T7-lycipi-IspA/pACT7-astaipi system, with a significant amount of β-carotene present across all the strains, evidence of a rate-limiting step in the pathway.

Acknowledgements

Foremost, I would like to thank my supervisor, Dr. Valerie Ward, for her continued guidance, knowledge and support of my M.A.Sc research and studies through the last two years. I could not imagine having a supervisor more invested in the success of my project as her, and I was very fortunate to be in such a close and supportive research group.

I would like to thank all those in the Bio Group, especially Dr. Marc Aucoin, for his support and for taking interest in my research and providing valuable insight and ideas. I thank those in the Ward lab: Sepandar Malekghasemi, Caleb Seward, Derek Kabernick and Hamid Hamedaani, for helping to create a fun and dynamic research environment that I was very happy to be part of.

I would also like to thank the Aucoin, Legge and Chou labs for their permission and trust to use their lab spaces and equipment for my research.

Table of Contents

List of Figures

List of Tables

List of Acronyms

DCW: dry cell weight

DMAPP: dimethylallyl pyrophosphate

DXP: 1-deoxy-D-xylulose 5-phosphate pathway

FPP: farnesyl pyrophosphate

GGPP: geranyl-geranyl pyrophosphate

GPP: geranyl pyrophosphate

G3P: glyceraldehyde-3-phosphate

HPLC: high-performance liquid chromatography

IPP: isopentenyl pyrophosphate

IPTG: isopropyl β-D-1-thiogalactopyranoside

IUP: isopentenol utilization pathway

MEP: methylerythritol phosphate pathway

MVA: mevalonate pathway

ROS: reactive oxygen species

1 Introduction

Astaxanthin, or 3,3'-dihydroxy-β,β-carotene-4,4'-dione, is a red carotenoid belonging to the isoprenoid family of organic compounds. Used for its strong antioxidant properties, its applications range through multiple industries, including the pharmaceutical, nutraceutical, cosmetic and aquaculture industries (Ambati, Phang, Ravi, & Aswathanarayana, 2014). As of 2017, the market for astaxanthin and other carotenoid throughout these industries was valued between $1.5B to $1.8B (Barredo, García-Estrada, Kosalkova, & Barreiro, 2017). While astaxanthin production naturally occurs in many species, including yeast, bacteria and algae, current industrial production methods include the cultivation of the green microalga *Haematococcus pluvialis* and chemical synthesis. Both methods present their own challenges and limitations (Ambati et al., 2014). Specifically, *H. pluvialis* has a complex life cycle, grows slowly, and requires a two-stage cultivation process under high light intensity, which limits the maximum cell density that can be achieved and subsequently the productivity of the process. Chemical synthesis, while inexpensive, results in a mixture of stereoisomers that may have weaker anti-oxidant properties than the primary (3S, 3'S) astaxanthin produced by biosynthesis (G. Jiang et al., 2020). Furthermore, synthetic astaxanthin is not approved for human use and thus the naturally produced version is in greater demand (Park, Binkley, Kim, Lee, & Lee, 2018). Much effort has been directed at heterologous production of astaxanthin in industrial workhorses like *Escherichia coli* because of their fast growth rates and the ease of achieving high-density cultures with these species.

E. coli possesses the genes needed to synthesize up to farnesyl pyrophosphate (FPP) using its native MEP pathway (Chia-wei Wang, Oh, & Liao, 1999). To extend the pathway to produce astaxanthin in *E. coli*, the genes *crtE*, *crtI*, *crtB*, and *crtY* must be introduced to the cell, along with a β-carotene ketolase and hydroxylase (Park et al., 2018). While a multitude of ketolases and hydroxylases have been used, recent work has shown that the use of carotenoid-β-ring-4-dehydrogenase (*cbfd*) and carotenoid-4-hydroxy-β-ring-4-dehydrogense (*hbfd*), sourced from the flowering plant *Adonis aestivalis*, generates high-purity astaxanthin in *E. coli* (Cunningham & Gantt, 2011).

The wild-type MEP pathway present in bacteria and chloroplasts is a highly regulated pathway with very low flux (Kirby & Keasling, 2009). As a result, researchers have attempted to improve

isoprenoid production by engineering this pathway, along with the mevalonate (MVA) pathway present in the cytosol of plant cells, yeast, and animal cells, for the last 30 years (Jeong, Cho, Choi, Kim, & Lim, 2018). Recently, a synthetic pathway for isoprenoid production, called the isopentenol utilization pathway (IUP), was developed to circumvent the regulatory challenges and decouple this pathway from central metabolism (Chatzivasileiou, Ward, Edgar, & Stephanopoulos, 2018). This pathway consists of choline kinase (*ck*) and isopentenyl phosphate kinase (*ipk*), which converts isoprenol into IPP and prenol into DMAPP, the precursors to all isoprenoids. This pathway was found to increase lycopene production 11-fold and increase productivity to 1.7 mg/g·h when induced with 25 mM isoprenol. The pathways are summarized in **Fig. 1**.

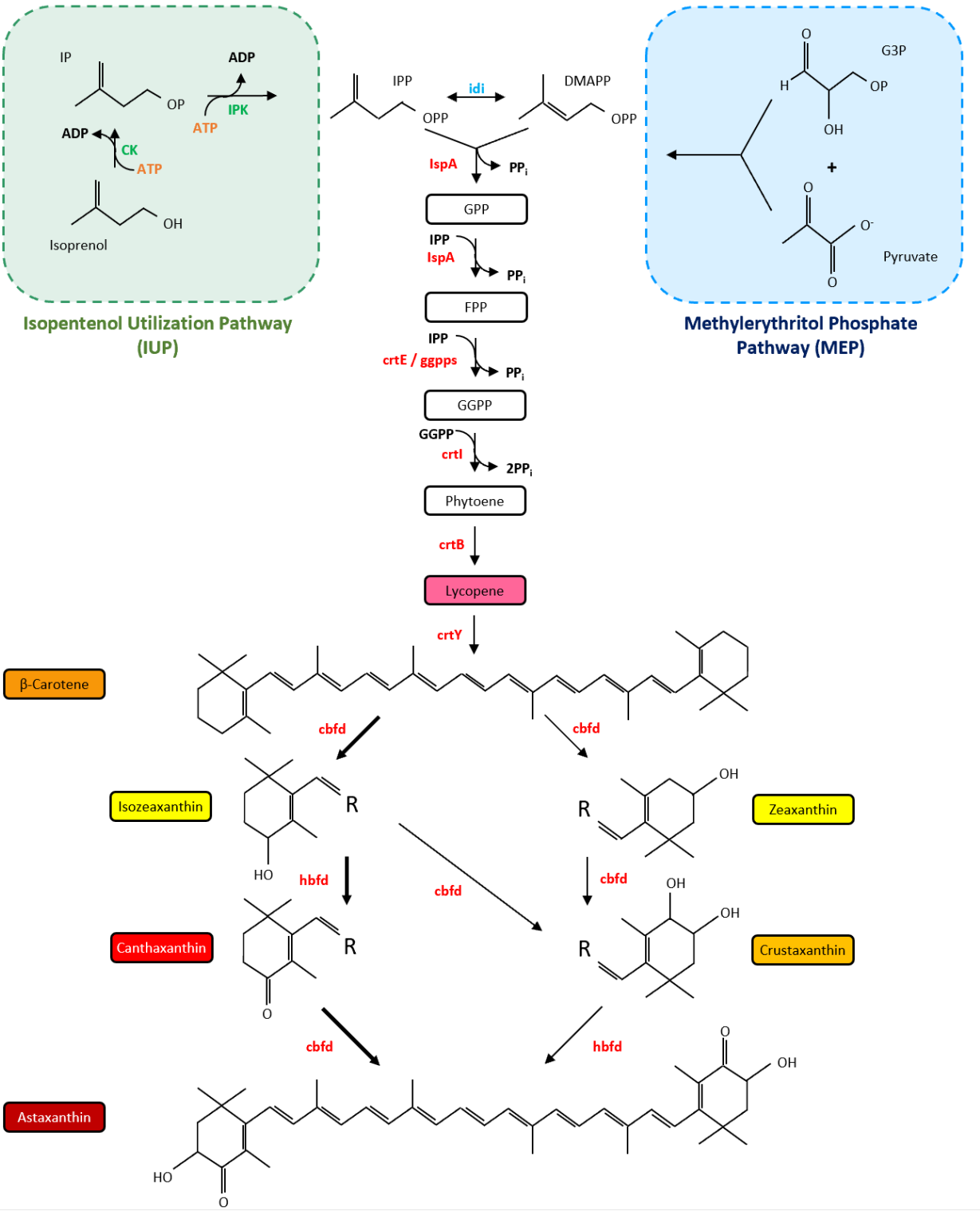

Fig. 1 – Astaxanthin biosynthesis pathways used in this study. The IUP pathway and its substrate, isoprenol is shown boxed in green, while the native MEP pathway and its precursors, glyceraldehyde-3-phosphate (G3P) and pyruvate, are boxed in blue. Darker arrows indicate the

preferred route of synthesis. A single β-ring structure is shown for each intermediate between β-carotene and astaxanthin as the enzymatic reaction occurs in a symmetrical fashion.

This thesis first outlines the previous reports of metabolic engineering of *E. coli* for carotenoid production, and the experiments performed to produce astaxanthin in *E. coli* using plasmid systems and genome integration containing the genes mentioned previously. The experimental methods that were used will be outlined in detail. In addition to simply producing astaxanthin, methods of enhancing production will be explored, including the upregulation of the MEP pathway, the inclusion of the IUP pathway, and the overexpression of *IspA*. The effect of media additives, including IPTG and casamino acids, will also be assessed. Carotenoid concentration and content will be calculated using absorbance readings and cell dry weight, and purity will be assessed using reverse-phase high-performance liquid chromatography.

2 Literature Review

2.1 Properties of Astaxanthin

Astaxanthin has the formula $C_{40}H_{52}O_4$ and a molar mass of 596.84 g/mol (Panis & Carreon, 2016). The abundance of functional groups in its structure allow for multiple sites for oxidation. This includes the many carbon-carbon double bonds along the main body of the molecule, as well as the carboxyl and hydroxyl groups on the β-ring at each terminal. As a result, astaxanthin is a strong antioxidant, with an oxidative strength that is many times higher than other carotenoids and antioxidants, such as β-carotene and vitamin C (Panis & Carreon, 2016). Astaxanthin, like all other isoprenoids, is derived from the root molecule isoprene, which is shown in **Fig. 2**. Isoprenoids exist in many plant species and act as aromatics, hormones, defense mechanisms and colouring agents (Kirby & Keasling, 2009). There is some evidence that supplementing astaxanthin in the human body can lower the risk of diseases caused by oxidative stress, such as cataracts disease, various cancers and diabetes (Zhang, Seow, Chen, & Too, 2018). Additionally, supplementation when ingested by mice did not exhibit any toxic effects (Lin, Lin, Wang, Chen, & Chiou, 2017). In the cosmetics industry, astaxanthin is used in various skin products, which make use of its vibrant red colour and antioxidant properties (G. L. Jiang, Zhou, Wang, & Zhu, 2017). Finally, in the aquaculture industry, astaxanthin is used in salmon and shrimp feed to brighten the colour of farmed fish and shrimp meat and create a more appealing product to be better sold in stores (Ambati, Phang, Ravi, & Aswathanarayana, 2014).

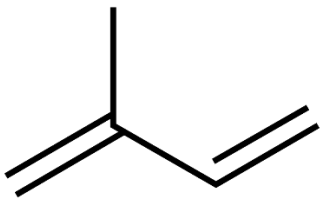

Fig. 2 – Molecular structure of isoprene. This acts as a repeating unit to form higher order isoprenoids, including all carotenoids.

2.2 Natural Astaxanthin Producers

Astaxanthin is produced by several species of algae, plants and yeast, and it is also accumulated in the flesh of fish and the shells of various shellfish, such as crab and lobster, through their diets

(Ambati et al., 2014). The astaxanthin present in chitin of shellfish is difficult to extract, so the most commonly used organism to produce astaxanthin in the biomanufacturing industry is the green microalga *Haematococcus pluvialis* (Boussiba, 2000). However, this species of microalgae has a very complex life cycle, as the cells go through several changes in form and development, which is illustrated in **Fig. 3** (Bauer & Minceva, 2019; Shah, Liang, Cheng, & Daroch, 2016).

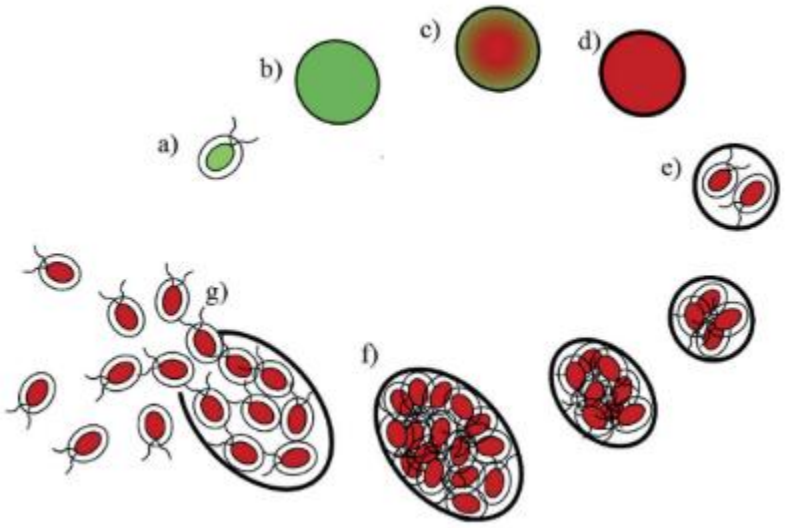

Fig. 3 – The stages of the life cycle of *H. pluvialis*. Astaxanthin is only formed under stressful conditions once the cells reach the flagellated stage. Retrieved from (Bauer & Minceva, 2019), permission requested.

Starting as a single cell inoculating a culture, it develops into a cluster of 32 cells, before germinating and splitting into individual flagellated cells, which become motile (Boussiba, 2000; Shah et al., 2016). Once conditions become harsh through a number of environmental stressors like high light intensity, they enter a vegetative state and develop into aplanospores, which accumulate astaxanthin within the cell in large cysts (Z. Gao et al., 2013). During this process, photosynthesis has been shown to decrease (Boussiba, 2000). Astaxanthin production can be induced through a lack of nutrients, high salinity or strong illumination. All these factors can be controlled using a photobioreactor, which is commonly used in industrial astaxanthin production (Kaewpintong, Shotipruk, & Powtongsook, 2007). Because high light intensity is often used to induce astaxanthin production and the growth rate of *H. pluvialis* is approximately 0.17 – 0.32 d^{-1}, a two-step cultivation with long residence times limits astaxanthin productivity (Olaizola, 2000). Further, astaxanthin that forms in *H. pluvialis* predominantly exists in an esterified form, and an

additional hydrolysis step would be necessary to remove the ester group, which can also form unwanted by-products (Chou, Ko, Yen, Chen, & Shaw, 2019).

2.3 Chemical Synthesis of Astaxanthin

The most common method of industrial astaxanthin production is chemical synthesis, which is significantly cheaper than the biological method (Panis & Carreon, 2016). There are a few different methods used, including direct hydroxylation of canthaxanthin, or the conversion of lutein to zeaxanthin through an isomerization reaction, followed by an oxidation reaction to make astaxanthin (Batghare, Singh, & Moholkar, 2018). Another option is to use a double Wittig reaction to convert 2,7-dimethyl-2,4,6-octatrienedial and 3-methyl-5-(2,6,6-trimethyl-3-oxo-4-hydroxy-1-cyclohexenyl)-2,4-pentadienyltriphenylphosphonium salt to form astaxanthin (Krause, Paust, & Ernst, 1997). The structures for each of the reaction components are given in **Fig. 4**. However, a number of safety issues are presented when considering the use of a chemical reactor (P. Zhou et al., 2017), and there is little to no control over which stereoisomers of astaxanthin are formed (G. Jiang et al., 2020). Furthermore, while astaxanthin synthesized through chemical means can be used for supplementation in fish feed, it is not approved for human use (Capelli, Bagchi, & Cysewski, 2013). More importantly, synthetic astaxanthin has a much lower antioxidant activity than astaxanthin produced by biosynthesis (Capelli et al., 2013). Due to these limitations, it would be preferable to produce astaxanthin in a biological system that is not tied to a complex life cycle like that of *H.* pluvialis, such as a fast-growing organism and common industrial workhorse like *Escherichia coli*.

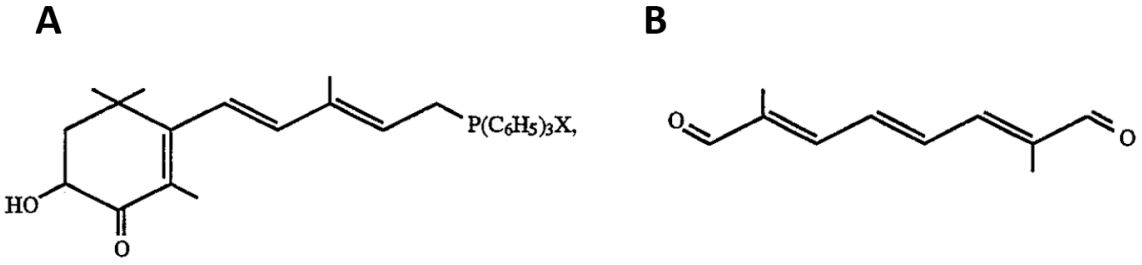

Fig. 4 – Structure of the reagents used in the double Wittig reaction to make astaxanthin. **A:** Structure of the C_{15}-triarylphosphonium salt. Two of these molecules are used in a single reaction. **B:** Structure of the C_{10}-dialdehyde. One of these molecules is used in each reaction.

2.4 Astaxanthin Biosynthetic Pathway Genes

The astaxanthin biosynthetic pathway is preceded by the methylerythritol phosphate (MEP) pathway, which is also sometimes called the 1-deoxy-D-xylulose 5-phosphate (DXP) pathway or non-mevalonate pathway. In this pathway, glyceraldehyde-3-phosphate (G3P) and pyruvate, derived from central carbon metabolism, are converted into isopentenyl pyrophosphate (IPP) and dimethylallyl pyrophosphate (DMAPP) (Park et al., 2018; Ward, Chatzivasileiou, & Stephanopoulos, 2018), the precursors for all isoprenoids. The enzyme isopentenyl diphosphate isomerase (*idi*) regulates the equilibrium between these two compounds (Rad et al., 2012). *E. coli* naturally possesses the gene *IspA*, which encodes the enzyme farnesyl pyrophosphate (FPP) synthase. This gene performs two steps in series: first converting IPP and DMAPP to geranyl pyrophosphate (GPP), and then adding another IPP to form FPP. However, the remaining genes required to synthesize astaxanthin in *E. coli* must be provided. This includes the genes for GGPP synthase (*crtE*), phytoene synthase (*crtI*), phytoene dehydrogenase (*crtB*), lycopene cyclase (*crtY*), β-carotene ketolase (*crtW*) and β-carotene hydroxylase (*crtZ*) (Park et al., 2018). The *crtZ* and *crtW* genes are promiscuous enzymes that can work in random order since they each oxidize a different carbon atom on the β-ring terminals. The divergence and convergence in the biological pathway accounts for the formation of both canthaxanthin and zeaxanthin, among other carotenoids, as intermediates (Park et al., 2018).

The genes in this pathway that synthesize from FPP to β-carotene (*crtE, crtI, crtB, crtY*) are present in many microorganisms, with the most commonly used genes in the metabolic engineering of carotenoids originating from the bacteria *Pantoea agglomerans* (formerly known as *Erwinia herbolica*) and *Erwinia uredovora* (Breitenbach, Misawa, Kajiwara, & Sandmann, 1996; Park et al., 2018). The genes used thus far for the conversion of β-carotene to astaxanthin originate from a number of species. One reason for this is that the enzymatic reactions that follow the synthesis of β-carotene are thought to be the rate-determining steps towards astaxanthin formation (Chia-wei Wang et al., 1999). A β-carotene ketolase coded by the gene *crtW* is a common homolog of *bkt*, which is generally sourced from *H. pluvialis* (Breitenbach et al., 1996). The work done by Cunningham and Gantt (2011) isolated some alternatives of *crtZ* and *crtW* from the flowering plant *Adonis aestivalis*, whose astaxanthin-producing genes are labelled as carotenoid β-ring 4-dehydrogenase (*cbfd*) and carotenoid 4-hydroxy-β-ring 4-dehydrogenase (*hbfd*), respectively, and incorporated them into a new plasmid that converts β-carotene into astaxanthin (Cunningham &

Gantt, 2011). A comprehensive list of the most popular organisms from which the genes in the astaxanthin biosynthetic pathway were sourced is represented in **Table 1**.

Table 1 – List of the possible sources for the genes needed to convert FPP to astaxanthin in *E. coli*. Homologs of more common genes are paired with their respective homolog in parentheses.

Species	List of Genes	Reference
Adonis aestivalis	*cbfd (crtZ), hbfd (crtW)*	(Cunningham & Gantt, 2011)
Agrobacterium aurantiacum	*crtI, crtB, crtY, crtW, crtZ*	(Chia-wei Wang et al., 1999)
Archaeoglobus fulgidus	*gps (crtE)*	(Chia-wei Wang et al., 1999)
Bacillus licheniformis	*idi*	(Rad et al., 2012)
Brevundimonas sp.	*crtW*	(Ma et al., 2016)
Chlamydomonas reinhartdii	*bkt (crtW)*	(Park et al., 2018)
Erwinia uredovora	*crtE, crtI, crtB, crtY*	(Yokoyama, Shizuri, & Misawa, 1998)
Haematococcus pluvialis	*bkt (crtW)*	(Breitenbach et al., 1996)
Pantoea agglomerans	*crtE, crtI, crtB, crtY, crtZ*	(Q. Lu, Bu, & Liu, 2017)
Pantoea ananatis	*crtE, crtI, crtB, crtZ*	(Q. Lu et al., 2017)
Sphingomonas sp.	*crtE*	(Ma et al., 2016)
Taxus canadensis	*ggpps (crtE)*	(Chatzivasileiou et al., 2018)

2.5 Cultivation of Carotenoid-Producing Organisms

The growth conditions for astaxanthin-producing *E. coli* are not much different than standard procedures since carotenoid production is no longer tied to stress induction. LB media is the most commonly used growth media for all types of bacterial growth (Park et al., 2018). However, use of a minimal media is preferred for large-scale cultivation, considering its lower material cost (Chatzivasileiou et al., 2018; J. Gao, Atiyeh, Phillips, Wilkins, & Huhnke, 2013). Although traditional growth media contains all the necessary nutrients for cell metabolism and carotenoid production by extension, the composition of the media can be changed in an attempt to enhance carotenoid production. The work done by Rad, Zahiri, Nogabi et al. (2012) examines the effect of different carbon sources on the production of lycopene when supplemented into LB media. The carbon sources that were studied include mannose, arabinose, fructose, acetate and citrate. The results from their experiments were insightful. Supplementing the media with 0.5% citrate was found to be beneficial for both cell growth and lycopene production. While cell growth was

relatively constant for most carbon sources with the exception of fructose, all the other carbon sources besides citrate had inhibitory effects of varying degrees on carotenoid production, as shown in **Fig. 5**. Arabinose, while inhibiting lycopene production, was shown to improve production of other isoprenoids, including perillyl alcohol, which is a product of limonene hydroxylation (Alonso-Gutierrez et al., 2013).

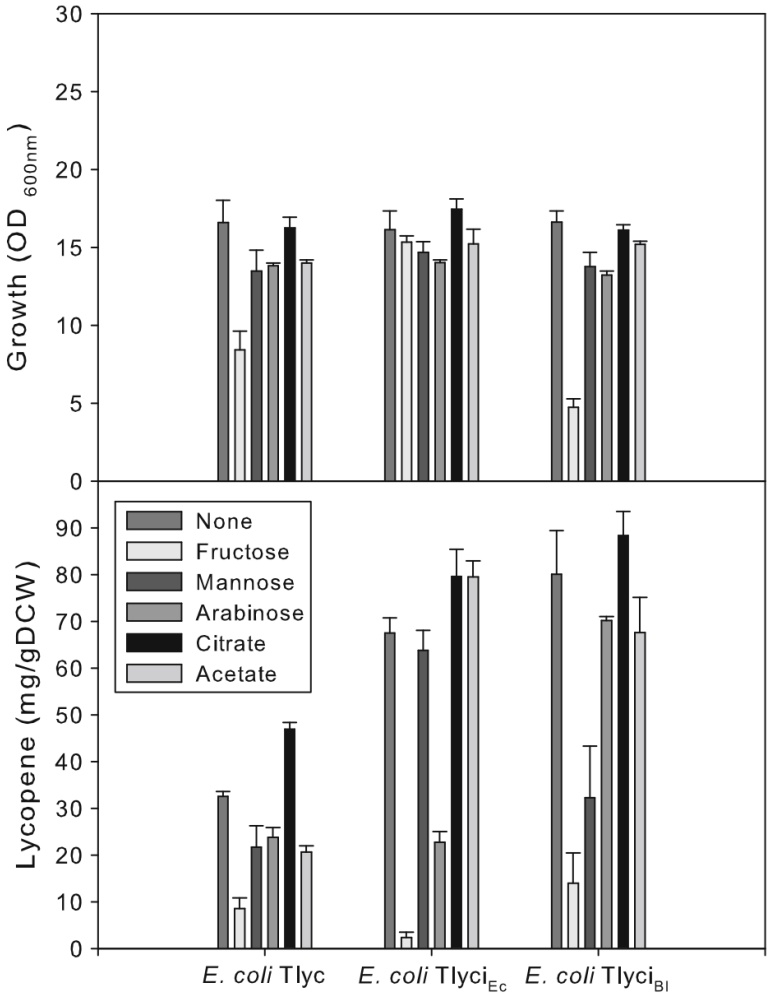

Fig. 5 – The effects of various alternative carbon sources on the production of lycopene, a precursor to astaxanthin. Using citrate had the greatest effect, while fructose had the most negative effect. Fructose also displayed growth inhibition. The three strains of *E. coli* used in this study have different lycopene-producing plasmids. Retrieved from (Rad et al., 2012), permission requested.

Subjecting carotenoid-producing cell cultures to sonication was found to increase astaxanthin production by changing the conformation of certain enzymes (Batghare et al., 2018). The conformation changes in the enzymes allowed for an increased metabolism at low to medium

sonication intensity, resulting in a 26% increase in volumetric astaxanthin concentration. Additionally, the formation of small bubbles through sonication promotes gas exchange in liquid media, which can increase the growth rate of the cultures. Increasing oxygen saturation has also shown to increase carotenoid production, which can be used in tandem with sonication to increase surface area for gas diffusion (Breitenbach et al., 1996).

An additional advantage of using *E. coli* for carotenoid production is the ease of carotenoid extraction. Firstly, the cell membranes of bacteria are easy to lyse compared to that of green algae and other plant cells, mainly due to the lack of a cell wall. Since carotenoids are hydrophobic, they accumulate inside the cell membrane so typical cell lysing agents and organic solvents such as ethanol and acetone work well at extracting and dissolving carotenoids (Ye et al., 2018). This extraction method also allows for the use of reverse-phase liquid chromatography, which is the most reliable method to determine specific carotenoid concentrations as well as the types of carotenoids in each sample (M. Lu, Zhang, Zhao, Zhou, & Yu, 2010). However, carotenoid extraction only from the cellular biomass does not account for carotenoids present in the liquid media. Simultaneous cultivation and extraction was used to extract carotenoids from the media improving carotenoid recovery by 43% (Zhang et al., 2018).

2.6 Metabolic Engineering of Astaxanthin Production

While introducing the necessary genes in the astaxanthin biosynthetic pathway will produce reasonable quantities of astaxanthin, higher quantities can be produced through various metabolic engineering strategies. This includes overexpression of pathway genes and the use of the CRISPR-Cas9 system to perform inserts or knockouts of genes to increase the flux towards astaxanthin production (Li, Lin, Huang, Zhang, & Wang, 2015). Other work has added modifications and tags to various enzymes to either mutate, fuse or localize them to specific locations within the cells to improve their activities (Henke & Wendisch, 2019; Chonglong Wang, Zada, Wei, & Kim, 2017).

2.6.1 Gene Overexpression

A simple yet effective way of increasing pathway flux and productivity is by gene overexpression. Of all the genes in the astaxanthin biosynthetic pathway, isopentenyl diphosphate isomerase (*idi*) is most commonly overexpressed, with a copy of this gene added to many carotenoid-producing plasmids (Jeong et al., 2018). Since this gene is naturally expressed in *E. coli*, only one extra copy is added onto a plasmid (Park et al., 2018). Adding an extra copy of *idi* has proven to be effective

strategy for increasing carotenoid production. One such experiment conducted by Rad et al. (2012) examined the effect of *idi* overexpression sourced from either *E. coli* or *Bacillus licheniformis*. Their results showed that the *idi* from *B. licheniformis* (type II) resulted in a greater improvement of lycopene production than *idi* from *E. coli* (type I), referring back to **Fig. 5**, even though production was greatly improved regardless of which *idi* gene was overexpressed (Rad et al., 2012). The significance of *idi* overexpression has also been assessed in comparison with *IspA* and *crtE* to determine which of the three genes had the most influence on the astaxanthin production rate, with *idi* being the most influential (Chia-wei Wang et al., 1999). The expression levels of *crtY* were also studied, as it was hypothesized that lycopene cyclization was a rate-limiting step, since lycopene was detected in their liquid chromatography analysis (Q. Lu et al., 2017). The addition of another copy of *crtY* not only increased the astaxanthin concentration to 7.4 mg/g in *E. coli*, but it also increased the purity from 92.6% to 96.6% astaxanthin (Q. Lu et al., 2017). The *crtB* and *crtI* genes were also overexpressed in other works, which also increased carotenoid production (Henke & Wendisch, 2019). The overexpression of genes in the upstream MEP pathway has also been examined. The work done by Matthews and Wurtzel (2000) determined the effect of overexpressing deoxyxylulose phosphate synthase (*dxs*), which is the first gene in the MEP pathway that synthesizes IPP and DMAPP (Matthews & Wurtzel, 2000). Through several experiments, they found that lycopene concentration increased by a factor of up to 10.8 and zeaxanthin concentration increased by a factor of up to 3.9 when an extra copy of *dxs* was added. Further, the introduction of an extra copy of the entire MEP pathway, sourced from *Kocuria gwangalliensis*, has been shown to increase astaxanthin concentration by a factor of 3 (Jeong et al., 2018).

Promoters play an important role in regulating gene expression, with some promoters having stronger expression levels than others. It is possible to change the promoter that regulates a gene's transcription levels so that it can be more strongly expressed. T5 and T7 promoters are popular for their naturally high expression levels and the strong inducing ability of isopropyl-β-D-1-thiogalactopyranoside (IPTG). Additionally, transcriptional regulators such as AppY have been implemented to upregulate carotenoid production (Chonglong Wang et al., 2017). Some works, including the experiments by Yuan et al. (2006), replaced the endogenous promoter responsible for transcribing several upstream genes, including *idi*, *dxs*, *IspB* and *IspF*, with a T5 promoter using CRISPR-Cas9 gene editing, which increased β-carotene concentration by a factor of 6.3 to

a value of 6 mg/g (Yuan, Rouvière, LaRossa, & Suh, 2006). Chou et al. (2019) also studied the effect of adding additional promoters onto astaxanthin-producing plasmids in between gene segments to boost production. Their designs contained a T7 promoter as well as two or three additional constitutive promoters in various layouts, as shown in **Fig. 6** (Chou et al., 2019). This practice has also been applied on the plasmid pCBFD1/HBFD1Bad, used in this work, which contains one promoter for *cbfd* and another for *hbfd* (Cunningham & Gantt, 2011).

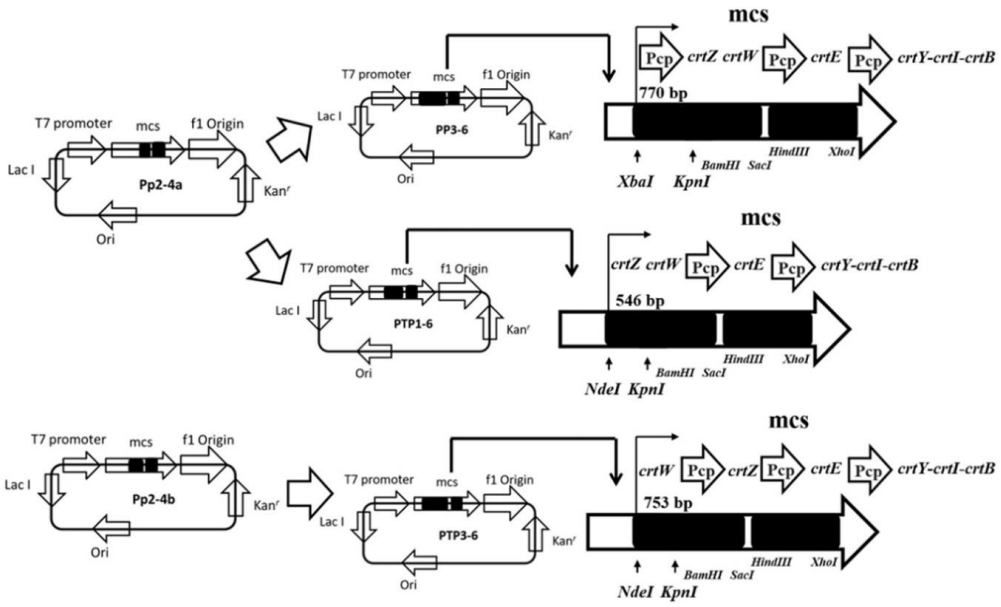

Fig. 6 – Plasmid design to produce astaxanthin with the use of additional constitutive promoters, labelled as Pcp. Retrieved from (Chou et al., 2019), permission requested.

From this experiment, the results showed that the best performing plasmid contained additional constitutive promoters for *crtZ* and *crtW*, supporting a need for a balance between the expression of these two genes. This plasmid yielded an astaxanthin concentration of 6.6 mg/g when induced with IPTG, and 3.3 mg/g without induction (Chou et al., 2019). Using the BL21 strain of *E. coli*, which is engineered for gene expression using T7 RNA polymerase, this value was increased to 8.32 mg/g. Editing the promoter region can be performed to achieve the opposite effect as well. This can be used on genes that compete for resources to downregulate their transcription and increase the flux through the astaxanthin biosynthetic pathway (Ribeiro, Tramontin, Kildegaard, Sudarsan, & Borodina, 2019).

2.6.2 CRISPR-Cas9 Gene Editing

Using CRISPR-Cas9 gene editing can reduce the metabolic burden of maintaining the genes in the astaxanthin production pathway on plasmids by inserting them directly into the *E. coli* genome. Additionally, inserts and deletions of other genes can increase carotenoid production by blocking certain parts of central carbon metabolism such that more resources go towards the MEP pathway. The work done by Li et al. (2015) tested this by knocking out and inserting genes that contribute to central carbon metabolism to improve β-carotene production in *E. coli*. They looked at deleting three genes individually as well as together: *ptsHIcrr*, which phosphorylates glucose to make glucose-6-phosphate, *gdhA*, which codes for glutamate dehydrogenase and makes glutamic acid, and *pykF*, which codes for pyruvate kinase and forms pyruvate. The three deletions are shown in **Fig. 7** as red X marks. The deletion of these genes would allow for greater flux through the MEP pathway (Li et al., 2015). From these experiments, they found that deleting *pykF* had the best outcome, as it resulted in the largest improvement in carotenoid production. The deletion of *ptsHIcrr* combined with the addition of an extra copy of *galP* also improved production. Although these two genes perform the same function, it is possible that one of these genes has a higher expression level. However, when all three deletions were performed at once, there was a decrease in both cell growth and in β-carotene production (Li et al., 2015).

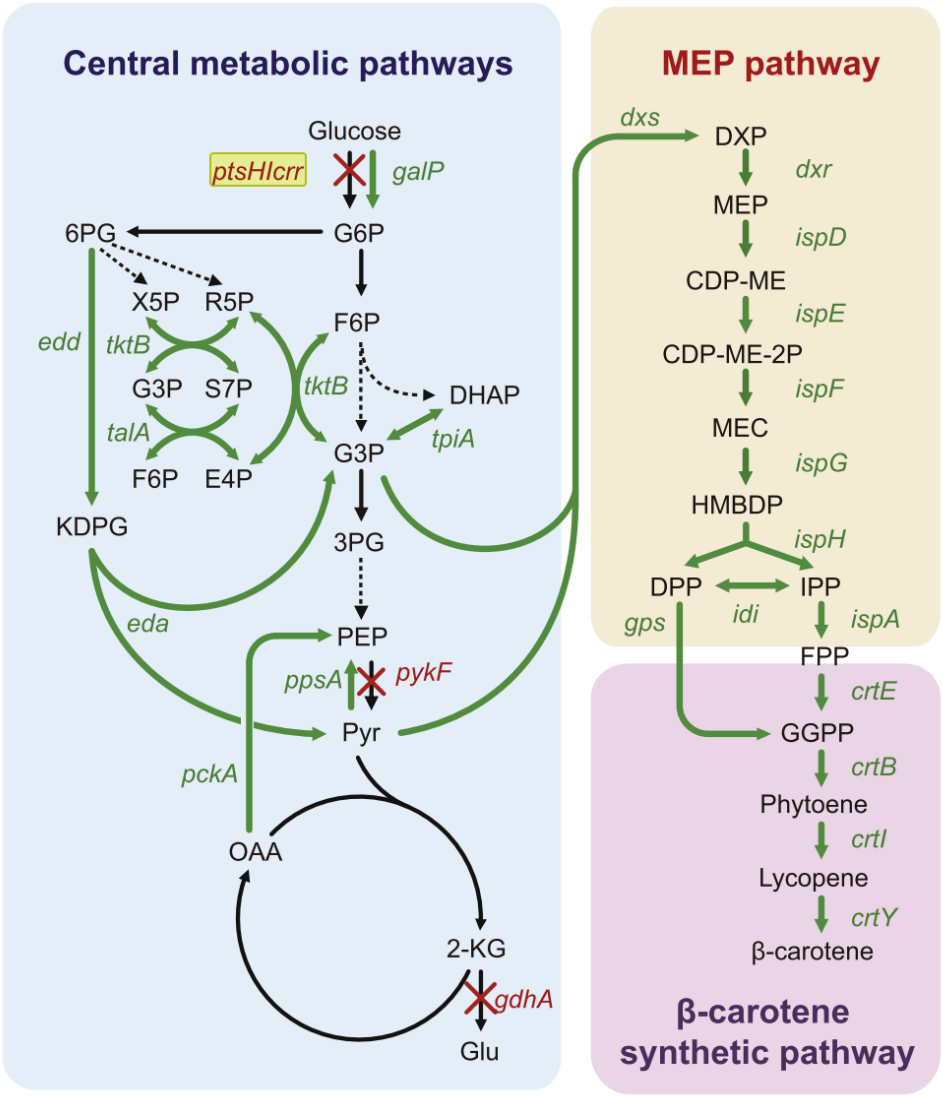

Fig. 7 – Central carbon metabolic pathway, showing the precursors to the astaxanthin biosynthetic pathway up to β-carotene. The arrows that are crossed out indicate the CRISPR knockout sites. Retrieved from (Li et al., 2015), permission requested.

Experiments in other works have looked at carotenoid production in pre-engineered strains of *E. coli* that already have gene knockouts. The paper by Zhou et al. (2013) produced lycopene in cell lines that had knockouts of *gdhA*, *zwf* and *pgi*, where *zwf* and *pgi* both code for glucose-6-phosphate dehydrogenase. Compared to their control with no knockouts, the *zwf* strain produced the most lycopene, with 2.3 times more lycopene, with a maximum concentration of 2.52 mg/g (Y. Zhou et al., 2013). However, this strain had a slower growth rate than the rest.

2.6.3 Gene Mutation

Mutation techniques have been used to enhance the activity of certain genes. While most of this work was done in yeast and algae, the methods used could be applied to *E. coli*. One of the methods used was irradiation using plasma and hydrogen peroxide treatments (G. Jiang et al., 2020). The results of the mutation were mainly qualitative, where the yeast colonies with the deepest red colour were selected as the best astaxanthin producers and were later grown up into cultures. Later testing showed an increase in carotenoid concentration by a factor of 2 after the treatment, as well as an increase in purity from 27% to 68%. The other method used low-fidelity PCR to induce random DNA replication errors (P. Zhou et al., 2017). A mutant library was created for the *bkt* gene using this technique. The most successful mutation resulted in an increase in carotenoid concentration by a factor of 2.33. In other cases, ultraviolet radiation and other mutagenic chemicals were used to induce mutations in yeast (M. Lu, Zhang, Zhao, Zhou, & Yu, 2010).

2.6.4 Protein Fusion and Localization

Another strategy to increase the local concentration of substrates for slow enzymes include fusing enzymes that perform subsequent steps together. The *crtZ* and *crtW* genes have been fused in this manner, since the conversion of β-carotene to astaxanthin is considered to be the rate-limiting step in the astaxanthin biosynthetic pathway (Chonglong Wang et al., 2017). The fusion protein GlpF has been used to link the two proteins (Henke & Wendisch, 2019) and DNA linkers of varying sizes have been studied to determine the ideal linker length (Nogueira et al., 2019). The paper by Nogueira et al. (2019) determined that fusing *crtZ* and *crtW* together using DNA linkers increased astaxanthin concentration by a factor of 1.3 and reduced the concentration of intermediates such as zeaxanthin and canthaxanthin by 20% (Nogueira et al., 2019). Using the GlpF fusion protein has been shown to increase astaxanthin concentration by a factor of 2 in other works (Henke & Wendisch, 2019), as well as increase zeaxanthin concentration by a factor of 3.72 (Ye et al., 2018).

Most carotenoids are thought to accumulate in the cell membrane due to their hydrophobic nature, and for example, phytoene desaturase (*crtI*) activity requires the presence of a lipid membrane. As a result, various works have looked at ways to localize the enzymes in the astaxanthin biosynthetic pathway to the cell membrane to increase production efficiency. One way of doing this is by tagging the genes with sequences that will target them towards the cell membrane. Proteins that have been used to tag genes for this purpose include the fusion protein GlpF and the signalling

proteins OmpF and TrxA (Park et al., 2018; Ye et al., 2018). This resulted in an increase in astaxanthin concentration by factors ranging from 2.08 to 3.15, based on various experiments (Park et al., 2018; Ye et al., 2018). Fluorescent tags can also be attached to proteins to make them visible using fluorescence microscopy and to confirm the localization of a protein (Fradkov et al., 2002). Fluorescence microscopy has also been used to observe cell membrane activity and the formation of membrane vesicles, which can be applied to quantify carotenoid concentration in the cell membrane. Reactive oxygen species (ROS), which astaxanthin and other antioxidants are known to counteract, can also be viewed using fluorescence microscopy (G. Jiang et al., 2020). The decrease in fluorescence due to ROS degradation can give insight to the localization of carotenoid accumulation. Since it is believed that the cell membrane can become oversaturated with carotenoids, which limits production, to combat this issue, efflux pumps such as AcrAB-TolC have be overexpressed to drive carotenoids out of the cell and into the liquid phase (Chonglong Wang et al., 2017).

2.6.5 Introduction of Alternative Upstream Pathways

Since the MEP pathway is not the only biological pathway in nature that feeds into the astaxanthin biosynthetic pathway, other non-native isoprenoid pathways can be introduced into *E. coli* to increase flux towards isoprenoid production. The MVA pathway, as the only other alternative natural isoprenoid pathway in nature, has also been introduced into *E. coli* for carotenoid production. The introduction of the MVA pathway increased lycopene content from 88 mg/g in the wild-type *E. coli* to 192 mg/g (Rad et al., 2012). Similar successes were seen with astaxanthin (Q. Lu et al., 2017).

Alternatively, Chatzivasileiou, Ward, Edgar and Stephanopoulos (2018) developed a novel synthetic pathway called the isopentenol utilization pathway (IUP) which is decoupled from central carbon metabolism since it uses exogenously fed isopentenol as a substrate rather than G3P, pyruvate, or acetyl-CoA like the MEP and MVA pathways. This pathway consists of choline kinase (*ck*) derived from *Saccharomyces cerevisiae*, and isopentenyl phosphate kinase (*ipk*) from *Arabidopsis thaliana*. These genes convert 3-methylbut-3-en-1-ol, or more commonly known as isoprenol, to IPP in two steps (or its isomer prenol to DMAPP), which directly feeds into the astaxanthin biosynthetic pathway (Chatzivasileiou et al., 2018). The IUP pathway was initially shown to be an effective replacement for the MEP pathway in a strain of *E. coli* containing a

knockout of *IspG*, disrupting the MEP pathway. However, because isoprenol is volatile, strains dependent on the IUP as an essential pathway are difficult to maintain. Addition of the IUP pathway using a plasmid in wild-type *E. coli* MG1655 (DE3) showed a significant increase in lycopene production, with concentrations reaching 8 mg/g at their maximum, while the control group was in the range of 1 mg/g. However, the flux through the pathway was calculated to be 11 times higher than any other reported flux for lycopene production, which was a significant improvement in isoprenoid production. In this work, the authors also investigated the effect switching *crtE*, derived from *Pantoea agglomerans*, to *ggpps*, a homolog with higher turnover from *Taxus canadensis* as the rate-limiting step was found to be formation of GGPP. The incorporation of *ggpps* improved productivity, although the final lycopene titre was similar for both scenarios, as seen in **Fig. 8**.

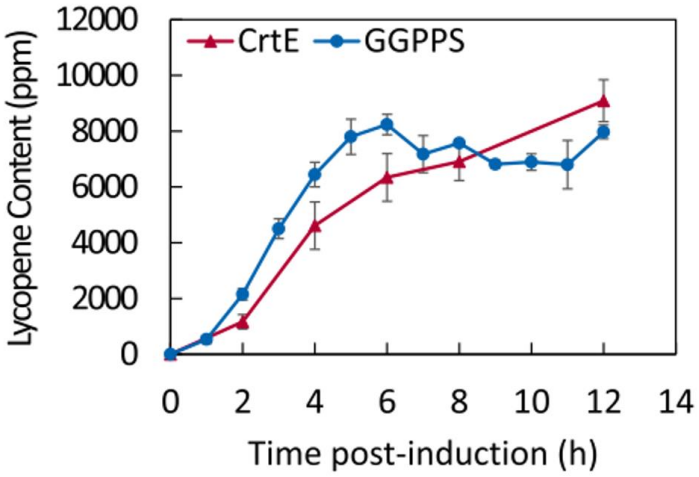

Fig. 8 – Lycopene production when comparing the use of *crtE* and *ggpps* as the gene coding for phytoene synthase. Even though the maximum concentration is similar between each sample, using *ggpps* results in a higher productivity. Retrieved from (Chatzivasileiou et al., 2018).

These past experiments in carotenoid production provide another comparison for astaxanthin production in this study. A list of previously obtained values for astaxanthin content, as well as the genes used to achieve them, are listed in **Table 2**.

Table 2 – List of astaxanthin-producing systems in *E. coli* from previous experiments and their resultant astaxanthin contents.

Gene Information – Source (Genes)	**Astaxanthin Content (mg/g)**	**Reference**
P. anantis (crtEIBYZ), Synthetic source (*trCrBKT-OmpF*)	5.68 ± 0.68	(Park et al., 2018)
P. anantis (crtEIBYZ, extra *crtY), Brevundimonas sp. (crtW)*	7.4 ± 0.3	(Q. Lu et al., 2017)
P. agglomerans (crtEIBY), A. aestivalis (cbfd, hbfd)	N.D., >99% purity	(Cunningham & Gantt, 2011)
E. uredovora (crtEIBYZ), A. aurantiacum (crtW)	4.2	(Yokoyama et al., 1998)
S. cerevisiae (hmgS, hmgR, mevK, pmk), E. coli (idi, atoB), P. agglomerans (crtEIB), P. anantis (crtYZ) Brevundimonas sp. (crtW)	10.0	(Zhang et al., 2018)
E. uredovora (crtEIBYZ), A. aurantiacum (crtW)	6.60	(Chou et al., 2019)
CAR003 genome *(crtEIBY), Brevundimonas sp. (crtW-GlpF), P. agglomerans (crtZ-GlpF)*	0.27 ± 0.04	(Ye et al., 2018)
K. gwangalliensis (dxs, ispCDEFGH, idi), P. haeundaensis (crtEIBYZW)	1.10 ± 0.05	(Jeong et al., 2018)
A. fulgidus (gps), A. aurantiacum (crtIBYZW)	1.25	(Chia-wei Wang et al., 1999)

3 Materials and Methods

3.1 Media Formulation

3.1.1 Luria-Bertani (LB) Media

To make LB media for bacterial growth, 10 g of sodium chloride, 10 g of tryptone and 5 g of yeast extract were added to 1 L of distilled water. The mixture was autoclaved to sterilize. When making LB plates, 15 g of bacteriological agar was added for every 1 L of media before autoclaving. To ensure the agar powder is well mixed, the media is agitated while still hot from the autoclaving. Once cooled to 50°C, antibiotic stocks were added if necessary, and the mixture was poured onto several petri dishes and stored at 4°C.

3.1.2 M9 Media

To make M9 media, several stock solutions must be prepared first. This includes a 20% w/w glucose stock, a 1 M magnesium sulfate stock and a 1 M calcium chloride stock. Each of these stock solutions were sterilized, either by autoclaving or filter sterilization using 0.2 μm syringe filters. 10.5 g of M9 broth mix was added to 1 L of distilled water and autoclaved to sterilize. Once cooled, 16 mL of the glucose stock, 2 mL of the magnesium stock and 0.1 mL of the calcium stock were added, along with 10 mL of trace elements solution based on the formulation from ATCC (Wolfe & Fowler, 1945).

3.1.3 SOC Media

To make SOC media, 20 g of tryptone, 5 g of yeast extract, 0.5844 g of sodium chloride, 0.186 g of potassium chloride, 0.9521 g of magnesium chloride, 3.603 g of glucose and 1.2037 g of magnesium sulfate were added to 1 L of water and autoclaved to sterilize.

3.2 Strains, Plasmids and Genes

New plasmids were designed using the New England Biolabs (NEB) online assembly tool. Template plasmid maps and DNA sequences inputted into this tool were retrieved from the lab's database on Benchling. Plasmid maps can be found in **Fig. A 1** to **Fig. A 8**. The properties of each strain and the plasmids used in this study are listed in **Table 3**. Primers for Gibson assembly were designed according to the assembly tool and ordered through Integrated DNA Technologies. The template plasmids were isolated from their cell hosts using the GeneAid Mini Prep kit and eluted in ultra-pure water. The Phusion high-fidelity PCR kit and protocol was used to amplify

the desired DNA fragments for the assembly. The primers used for this process are given in **Table A 1**. If the desired fragment was similar in size to the template plasmid, 1 μL of DpnI was added to the reaction mixture and incubated at 37°C for 1 h. The fragments were recovered using agarose gel electrophoresis for 1 h at 90 V. A razor blade was used to cut the band out of the gel, and the GeneAid Gel Extraction kit was used to purify the DNA and elute it in ultra-pure water. The fragments for each assembly were quantified using a Nanodrop to obtain mass and molar concentrations. The Gibson assembly mixture was made by adding 5 μL of NEB Hi-Fi assembly master mix, backbone DNA solution such that 50 ng to 100 ng of backbone was present in the assembly mixture, the correct molar ratio of the other fragments (1 mol backbone : 1 mol fragment for 4 or more fragments, 1 mol backbone : 2 mol fragment for smaller assemblies), and filled to 20 μL with ultra-pure water. The mixture was incubated for 1 h at 50°C and stored at -20°C for use. Newly assembled plasmids were transformed into chemically competent NEB-5α cells using heat shock. Colony PCR was used to confirm the correct assembly of the DNA fragments. Diagrams of the constructs used in this project is given in **Fig. 9**.

Table 3 – The bacterial strains, genes and plasmids used in this study.

Host/Strain	**Description**	**Reference**
MG1655(DE3)	Δ*endA* Δ*recA* (λ DE3)	(Ajikumar et al., 2010)
MG1655(DE3)-trcMEP	Δ*endA* Δ*recA* (λ DE3) P_{trc} *dxs-idi-ispDF*	(Ajikumar et al., 2010)
NEB-5α	*fhuA2 Δ(argF-lacZ)U169 phoA glnV44 Φ80 Δ(lacZ)M15 gyrA96 recA1 relA1 endA1 thi-1 hsdR17*	NEB
Plasmids	**Description - Origin, antibiotic marker, promoter (operon)**	**Reference**
pAC-BETAipi,	Cm^R, P_{endo} (*crtE, ipi, crtY, crtI, crtB*)	Addgene [#53277]
pCBFD1	Ap^R, P_{BAD} (*cbfd*), P_{lac} (*hbfd*)	Addgene [#53364]
pSEVA228-pro4IUP	RK2, Kn^R, P_{pro4} (*ck, ipk, idi)*	(Chatzivasileiou et al., 2018)
p5T7-lycipi-ggpps	pSC101, Sp^R, $P_{T7lacUV}$ (*ggpps, ipi, crtI, crtB*)	(Chatzivasileiou et al., 2018)
p5T7-astaipi-ggpps	pSC101, Sp^R, $P_{T7lacUV}$ (*ggpps, crtY, cbfd, hbfd, ipi, crtI, crtB*)	This study
p5T7-lycipi-IspA,	pSC101, Sp^R, $P_{T7lacUV}$ (*ggpps, IspA, ipi, crtI, crtB*)	This study
pACT7-astaipi	pSC101, Cm^R, $P_{T7lacUV}$ (*cbfd, crtY, hbfd*)	This study
Genes	**Origin (Accession Number)**	**Reference**
ck	*S. cerevisiae* (AAA34499.1), codon optimized	(Chatzivasileiou et al., 2018)
ipk	*Arabidopsis thaliana* (AAN12957.1), codon optimized	(Chatzivasileiou et al., 2018)
idi	*E. coli* (AAD26812.1)	(Rad et al., 2012)
IspA, ispD, ispF	*E. coli*	
dxs	*E. coli*	
ggpps	*Taxus canadensis* (AAD16018.1), codon optimized, truncated first 98 amino acids, methionine added	(Chatzivasileiou et al., 2018)
crtE, crtB, crtI, crtY, ipi	*Pantoea agglomerans*, *crtE* (AAA21260.1), *crtB* (AFZ89043.1), *crtI* (AFZ89042.1), *crtY* (AAA64980.1), *ipi* (AAA64978.1)	(Cunningham & Gantt, 2011)
cbfd, hbfd	*Adonis aestivalis*, *cbfd* (ABK41045.1), *hbfd* (AAV85452.1)	(Cunningham & Gantt, 2011)

Sp^R = spectinomycin, Kn^R = kanamycin, Ap^R = ampicillin, Cm^R = chloramphenicol

The *ggpps, crtB, crtI* and *idi* genes were amplified from p5T7-lycipi-ggpps. This plasmid was used as the backbone to make p5T7-astaipi-ggpps. The *crtY* gene was taken from pAC-BETAipi, and *cbfd* and *hbfd* were taken from pCBFD1. These plasmids were both purchased from Addgene (plasmid #53277 & #53364). For the upregulation of *IspA*, which was sourced from p5T7-IspA-ads, the gene was added to p5T7-lycipi-ggpps to make p5T7-lycipi-IspA, and a separate plasmid, pACT7-astaipi, was made to house the remainder of the pathway genes.

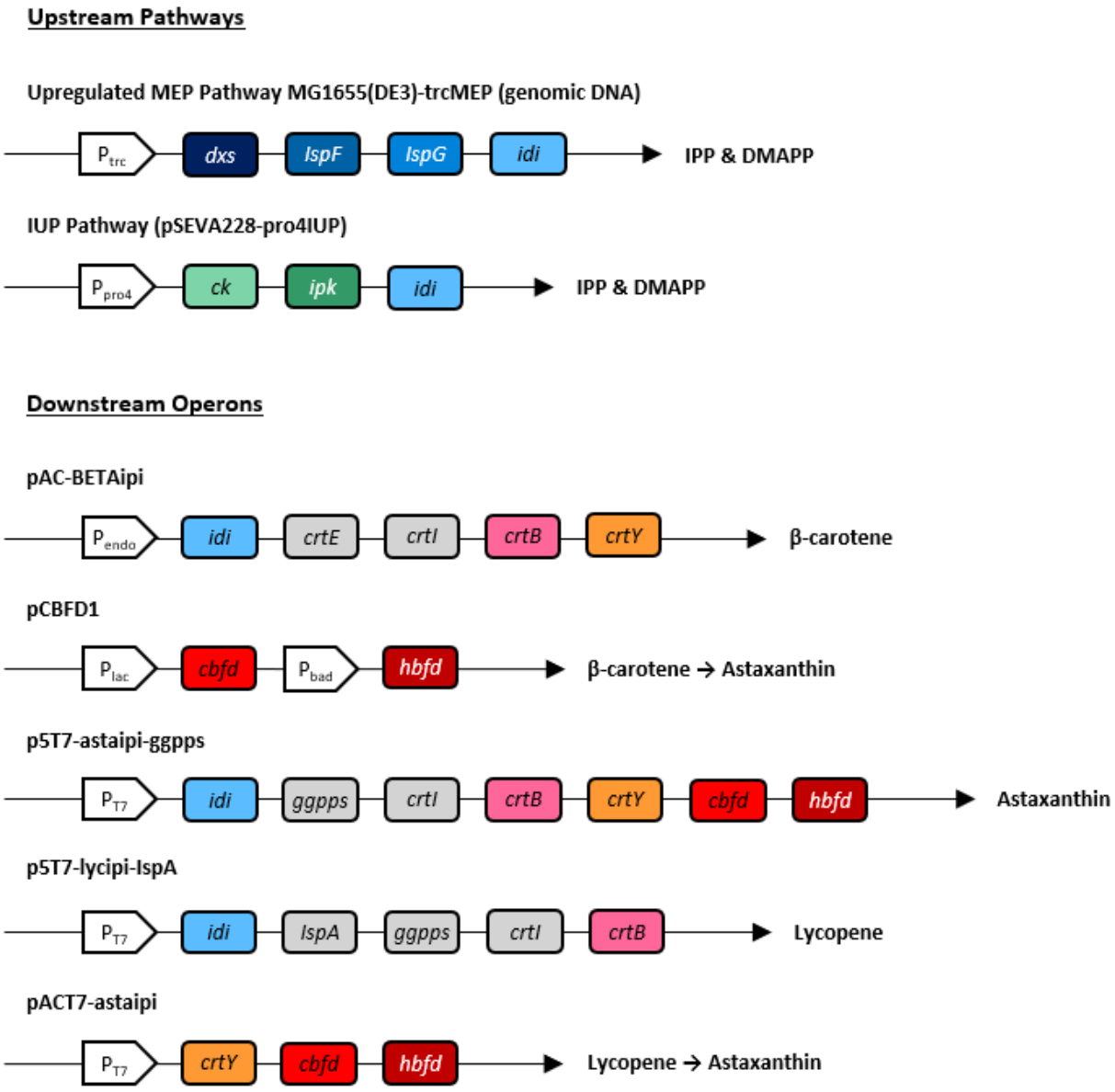

Fig. 9 – Plasmid designs for producing astaxanthin. The product of each plasmid is shown on the right. Plasmids that form intermediates in the pathway can be combined in one system to produce astaxanthin. The genes in both upstream pathways (trcMEP and IUP) are also shown.

3.3 Culture Conditions

Bacterial strains were grown in LB media to prepare frozen stocks or competent cells. Antibiotic stocks and inducer stocks were made at 1000 x concentration, and were filter sterilized for storage at -20°C. For experiments in carotenoid production, seed cultures were grown in M9 media at 30°C for 24 h, shaking at 200 rpm. The seed cultures were used to inoculate larger cultures at a

1% v/v inoculum and cultivated in triplicate in 50 mL batches of M9 media. Strains 1, 2 and 3 acted as positive controls to assess the productivity of the newly cloned plasmids. The appropriate antibiotics were used depending on the astaxanthin-producing plasmids present in each strain. At an OD_{600} of 0.5, carotenoid biosynthesis was induced using 0.1 mM IPTG (P_{T7} strains), 1 g/L arabinose (P_{BAD} strains) and 25 mM isoprenol (IUP strains). A list of the strains used in this project can be found in **Table 4**.

Table 4 – List of all the astaxanthin-producing strains of E. coli and their plasmid systems. The plasmid pCBFD1/HBFD1Bad was abbreviated to pCBFD1.

Strain	Host	Upstream Plasmid	Downstream Plasmid(s)
1	MG1655(DE3)	n.a.	pAC-BETAipi, pCBFD1
2	MG1665(DE3)-trcMEP	n.a.	
3	MG1655(DE3)	pSEVA228-pro4IUP	
4	MG1655(DE3)	n.a.	p5T7-astaipi-ggpps
5	MG1665(DE3)-trcMEP	n.a.	
6	MG1655(DE3)	pSEVA228-pro4IUP	
7	MG1655(DE3)	n.a.	p5T7-lycipi-IspA, pACT7-astaipi
8	MG1665(DE3)-trcMEP	n.a.	
9	MG1655(DE3)	pSEVA228-pro4IUP	

3.4 Carotenoid Extraction

Carotenoid content was assessed at the indicated time points post-induction. Two 1 mL samples were taken from each culture. The samples were all stored in amber microtubes to prevent photodegradation and were centrifuged at 15000 rpm for 1 min to isolate the cell pellet. One set of samples was resuspended in 1 mL of a 1:1 v:v ethanol-acetone solution and were left to incubate in the dark for 1 h at room temperature. After centrifuging the cell suspension again, 200 µL of the liquid phase was transferred to a 96-well plate. The absorbance at 475 nm was recorded for each time point using a BioTek® Synergy 4 well-plate reader. At the same time, a blank sample containing 200 µL of the ethanol-acetone solution was measured for absorbance. The second set of 1 mL samples were lyophilized and weighed to obtain the cell dry weight (g/L) at each time point. The following equation was used to convert absorbance units to carotenoid concentration per unit volume (mg/L), making use of the astaxanthin standard curve shown in **Fig. C 1**. This is

divided by the cell dry weight to obtain carotenoid content, the total carotenoid concentration per gram of biomass (mg/g).

$$Carotenoid\ Content\ \left(\frac{mg}{g}\right) = \frac{Absorbance - blank}{0.0799\ \left(\frac{L}{mg\ Asta.}\right)} \div Cell\ Dry\ Weight\ \left(\frac{g}{L}\right)$$

3.5 Analytical Procedures

The astaxanthin content of each producing strain was analyzed using reverse-phase high performance liquid chromatography (HPLC), using an Agilent® 1260 Infinity II chromatographer and a YMC Carotenoid column (C_{30}, 250 mm, 5 μm pore size). Samples and carotenoid standards were prepared in 1:1 v:v ethanol-acetone solution and stored in amber HPLC vials at -80°C, and at 4°C inside the loading chamber during the analysis. A mobile phase of 81:15:4 v:v:v MTBE: methanol: water was used for the first trial at a flowrate of 1.0 mL/min for 20 min per sample. For the second trial, two mobile phases were used, one with the same composition as the first trial (A), and the other consisting of 15:81:4 v:v:v MTBE: methanol: water (B). An elution gradient from 100% B to 100% A was implemented for 15 min, followed by 100% B for 12 min. A second elution gradient from 100% A to 100% B was used for another 3 min. The column was maintained at 20°C for the duration of these analyses. The HPLC results were calibrated according to carotenoid standards of astaxanthin, canthaxanthin, zeaxanthin, lycopene and β-carotene, shown in **Table C 2**.

3.6 Competent Cell Preparation

3.6.1 Electrocompetent Cells

Electrocompetent *E. coli* (WT or trcMEP) cells were made by first growing a 5 mL seed culture, inoculated from a pre-made glycerol stock. This was done in a sterile Falcon tube at 37°C and shaking at 250 rpm. During this time, a stock solution containing 20% v/v glycerol and 15 g/L of mannitol was made and autoclaved to sterilize. Once the culture reached maximum cell density, usually after a night of incubation, 200 mL of fresh LB media was inoculated with the seed culture such that the OD_{600} of the new culture was about 0.01. The culture, split into two 500 mL Erlenmeyer flasks, was incubated at 30°C and 200 rpm until the OD_{600} was between 0.4 and 0.6. The flasks were immediately placed on ice for 30 min to chill. The cultures were transferred to four 50 mL Falcon tubes and centrifuged at 4°C and 3720 rpm for 15 min. The cells were resuspended in 10 mL of cold water per tube and combined into two of the Falcon tubes. In each

tube, a 10 mL serological pipette was used to slowly pipette 10 mL of the glycerol and mannitol stock solution into the bottom of each tube. A small amount of solution was left in the pipette to avoid any disturbance and mixing of the two phases. The tubes were centrifuged again under the same conditions and resuspended in 200 μL of the glycerol and mannitol stock. The concentrated solution was aliquoted into 50 μL portions in sterile microtubes and stored at -80°C.

3.6.2 Chemically Competent Cells

Chemically competent cells were made using a 5 mL seed culture of NEB-5α cells, grown in LB media overnight at 37°C. During that time, a 0.1 M calcium chloride stock, a 0.1 M magnesium chloride stock and a 15% glycerol stock containing 85 mM calcium chloride were prepared and autoclaved, and stored at 4°C. Once the seed culture reached maximum cell density, 500 mL of LB media was inoculated with the entire seed culture at a 1% v/v inoculum. The culture was grown at 30°C, shaking at 200 rpm, until the OD_{600} reached between 0.35 and 0.4. The culture was then chilled on ice for 30 min and centrifuged in two large centrifuge bottles at 4°C and 3000 x g for 15 min. The bottles were each resuspended in 100 mL of the magnesium stock and separated into four 50 mL Falcon tubes. The tubes were then centrifuged at 2000 x g for 15 min. Each tube was resuspended in 50 mL of the calcium stock and left on ice for 20 min before centrifuging again. The cells were resuspended in 12.5 mL of the calcium and glycerol stock per tube and combined into one of the tubes before centrifuging at 1000 x g for 15 min. Finally, the cells were resuspended in 2 mL of the same stock solution and aliquoted into 50 μL portions and stored at -80°C.

3.7 Gel Casting

A large quantity of 1x TAE buffer was made by mixing 4.84 g of tris-base, 0.412 g of disodium EDTA dihydrate and 1.14 mL of glacial acetic acid in 1 L of ultra-pure water. The mixture was moderately heated to completely dissolve all the components. To make a 50 mL gel, 0.5 g of agarose was added to 50 mL of buffer and brought to a boil. Once cooled to 50°C, 2.5 μL of SafeView Classic was added to the mixture and mixed gently. The liquid was poured into the gel tray with a well comb in place and left to cool until the gel solidified.

3.8 Heat Shocking of Bacteria

One portion of chemically competent NEB-5α cells was thawed on ice, along with a plasmid suspension. Two microlitres of the plasmid mixture was added to the cells and flicked to mix.

The mixture was left on ice for another 30 minutes. The cells were then placed in a pre-heated water bath at 42°C for exactly 30 seconds and placed back on ice for exactly 2 min. Once the 2 minutes expired, 1 mL of SOC media was added to the cells, and the tube was incubated for 2 h at 37°C, shaking at 250 rpm. 100 μL of the cell culture was spread onto a LB agar plate containing the appropriate antibiotics and incubated at 37°C for 24 h.

3.9 Colony PCR

Successfully transformed colonies were grown up on another fresh LB agar plate. A small amount of cell mass from each colony was suspended in separate PCR tubes with 10 μL of sterile ultra-pure water and incubated at 98°C for 15 min. Taq DNA polymerase and standard Taq buffer, along with the Taq protocol, were used to amplify a section of the plasmid DNA, using a new pair of primers designed on PerlPrimer. One microliter of the cell suspension was used as a template for the reaction. Each reaction mixture was run on 1% agarose gel using the standard gel electrophoresis protocol. Of the colonies that displayed the correct band length, one was used to inoculate a 25 mL culture of LB media. This culture was grown overnight and used to Mini Prep the plasmid. Plasmids isolated after this step were sent to the Toronto Hospital for Sick Children's DNA sequencing facility for sequencing.

3.10 Electroporation of Bacteria

One portion of electrocompetent cells (WT or trcMEP) was thawed on ice, along with a plasmid suspension that has been correctly sequenced. Once thawed, the contents of the cell suspension were transferred to a chilled electroporation cuvette with a 1 mm gap. 1 μL of the DNA suspension was added to the cuvette as well. If there was more than one plasmid being transformed, 1 μL of each plasmid suspension was added. After ensuring that there were no bubbles in the suspension, the cuvette was placed inside an electroporation chamber and pulsed at 1.8 kV and 25 μF capacitance. 1 mL of SOC media was immediately added to the cuvette to resuspend the cells, and the entire mixture was transferred to a sterile tube and incubated at 37°C for 2 h. One hundred microlitres of the culture was spread onto a LB plate with the appropriate antibiotics and incubated at 37°C for 24 h. Successfully transformed colonies were used for glycerol stock preparation and future experiments.

4 Results and Discussion

4.1 Total Carotenoid Analysis

Strains were cultured under a number of different conditions. In all cases, cell density and carotenoid concentration were monitored approximately every 6-12 h. All experiments were conducted in triplicate and data is available in **Table B 1** – **Table B 11**.

First, in order to confirm astaxanthin production and compare the performance of the upstream pathways, the plasmids pAC-BETAipi and pCBFD1 were purchased from Addgene (Cunningham & Gantt, 2011) and were transformed into wild-type *E. coli* MG1655 (DE3) – Strain 1, *E. coli* MG1655 (DE3) containing an upregulated MEP pathway (trcMEP) – Strain 2, and the *E. coli* MG1655 (DE3) containing the IUP pathway plasmid – Strain 3. Strains were cultured in LB media and were induced at the time of inoculation. Since the IUP strain (Strain 3) is a triple-plasmid system, p5T7-astaipi-ggpps was made to decrease the overall metabolic burden on the cell by combining all the genes in the pathway into a single plasmid. At the same time, *crtE* was replaced with *ggpps* derived from *Taxus canadensis*, which has been shown to increase lycopene productivity compared to *crtE* (Chatzivasileiou et al., 2018).

Using either the IUP plasmid system or the trcMEP host strain resulted in decreased maximum cell density when either astaxanthin plasmid system was used (**Fig. 10A**). However, both sets of strains (1 – 3 & 4 – 6) reached similar total carotenoid concentrations and carotenoid content depending on which upstream pathway was used. The pAC-BETAipi/pCBFD1 system (Strains 1 – 3) generally had a higher maximum carotenoid concentration in each host. Upregulating the MEP pathway (Strains 2 & 5) had, on average, a greater effect than introducing the IUP pathway (Strains 3 & 6). Upregulating the MEP pathway increased total carotenoid production more than introducing the IUP pathway, although both methods increased the total carotenoid content, shown in **Fig. 10C**. The change in concentration when upregulating the MEP pathway and adding the IUP pathway was greater in the p5T7-astaipi-ggpps system because the carotenoid production decreased in the wild-type host. While the pAC-BETAipi and pCBFD1 strain had a 5.6-fold increase in concentration, up to 4.25 ± 0.04 mg/g dcw, with the upregulated MEP pathway, the p5T7-astaipi-ggpps strain had an 8.3-fold increase, up to 3.58 ± 0.22 mg/g dcw. Likewise, the increase in carotenoid content of the two strains with the IUP pathway were 3.2-fold for the pAC-

BETAipi/pCBFD1 system and 4.2-fold for the p5T7-astaipi-ggpps system, with final carotenoid content readings of 2.43 ± 0.21 mg/g dcw and 1.81 ± 0.35 mg/g dcw, respectively.

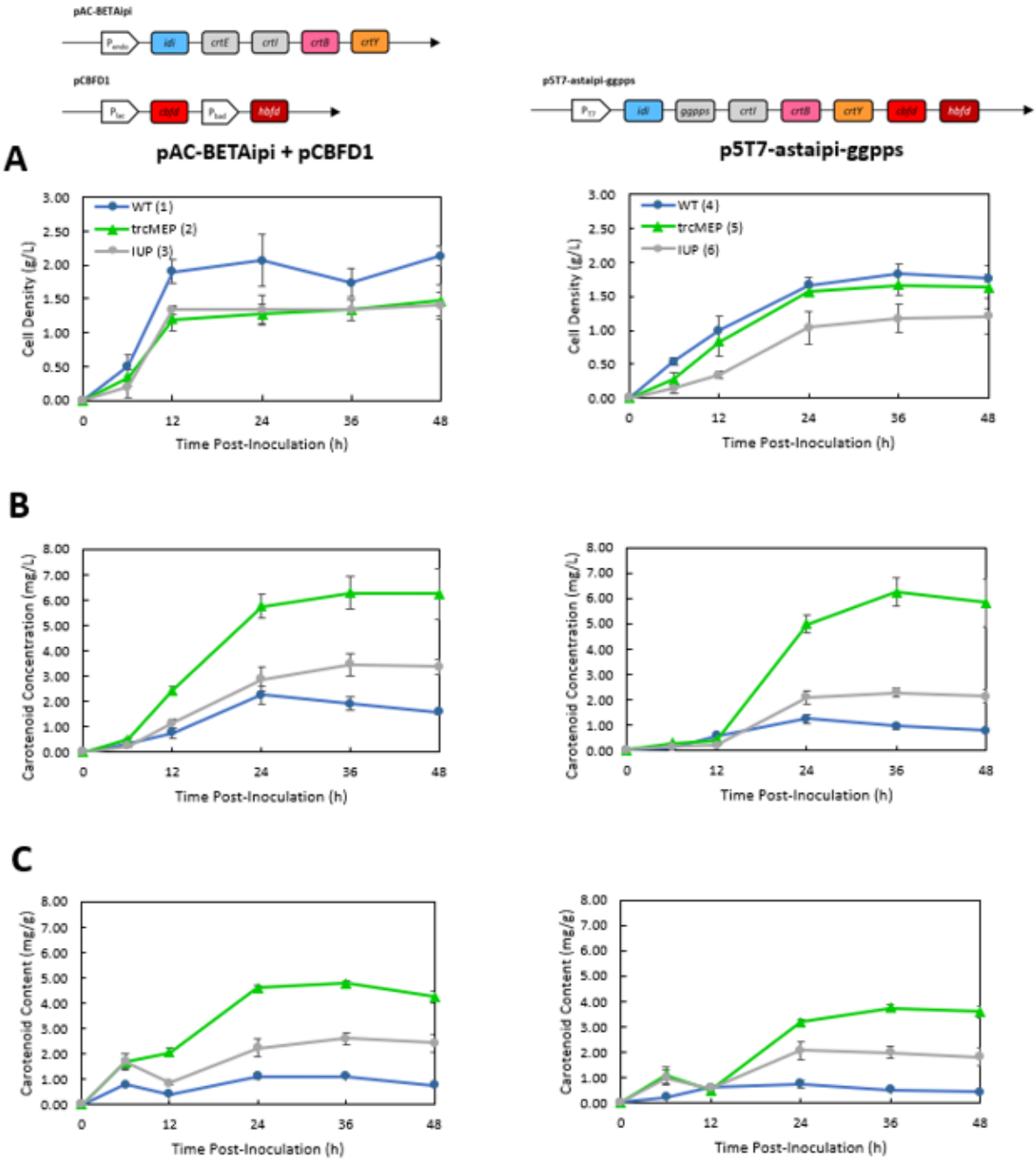

Fig. 10 – Growth profiles of Strains 1– 6 grown in LB media induced from the start of inoculation. **A:** Cell growth curves for Strains 1 – 6. **B:** Carotenoid concentration profiles for Strains 1 – 6. **C:** Carotenoid content profiles, as a function of cell density.

The productivity of each strain was calculated and is summarized in **Table 5**. Strain 2 and 5, which had an upregulated MEP pathway, had the highest productivity, which corresponds to their higher carotenoid contents.

Table 5 – Total carotenoids and productivity for the six strains in LB media. Productivity was calculated over 48 h.

Strain	Max. Cell Density (g/L)	Max. Carotenoid Conc. (mg/L)	Max. Carotenoid Content (mg/g)	Time (h)	Productivity (μg/g·h)
1	2.13 ± 0.15	2.25 ± 0.33	1.13 ± 0.34	48	23.5 ± 7.1
2	1.47 ± 0.23	6.27 ± 0.66	4.77 ± 0.90	48	99.4 ± 18.8
3	1.40 ± 0.20	3.45 ± 0.44	2.60 ± 0.43	48	54.2 ± 8.9
4	1.83 ± 0.15	1.23 ± 0.16	0.75 ± 0.14	48	15.6 ± 2.9
5	1.67 ± 0.15	6.25 ± 0.58	3.75 ± 0.13	48	78.1 ± 2.7
6	1.20 ± 0.26	2.28 ± 0.18	2.06 ± 0.37	48	42.9 ± 7.7

A second experiment was conducted to assess the effect of inducing the cells at an OD_{600} of 0.5 rather than from the time of inoculation and time profiles for these cultures are shown in **Fig. 11.** These cultures showed a similar trend as the first set of cultures, however, some carotenoid production was already evident at the time of induction as the pAC-BETAipi/pCBFD1 plasmid system uses a constitutive promoter to produce carotenoids up to β-carotene (Cunningham & Gantt, 2011). Growth was improved compared with later induction as seen in **Fig. 11A.** The carotenoid concentration and carotenoid content profiles, shown in **Fig. 11B-C**, were similar to the previous experiment, with the maximum carotenoid concentration accumulated for each strain unchanged. For the p5T7-astaipi-ggpps system, the carotenoid content improved slightly in the trcMEP strain, while the IUP strain had a small decrease. However, inducing the cells during exponential phase is more consistent with experiments from other works, and so this practice was adopted for all future experiments (Chatzivasileiou et al., 2018).

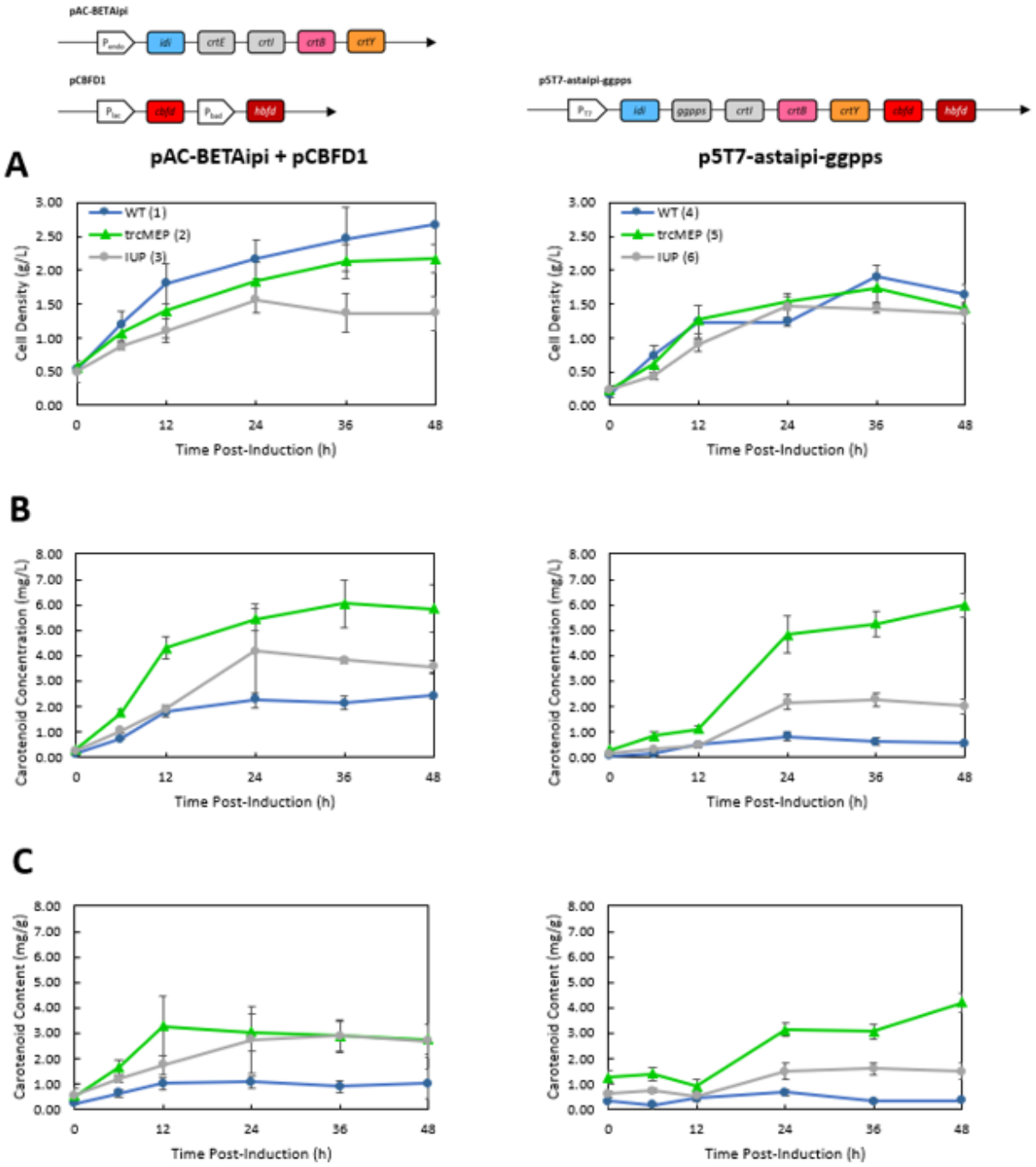

Fig. 11 – Concentration profiles for the first six *E. coli* strains in LB media, induced at an OD_{600} of 0.5. **A:** Cell growth curves for Strains 1 – 6. **B:** Concentration profiles for Strains 1 – 6. **C:** Carotenoid content as a function of cell density.

Under these conditions, similar to the first experiment, strain productivity was highest in Strains 2 and 5, containing the upregulated MEP pathway. These results are given in **Table 6**.

Table 6 – Total carotenoids and productivity of the six strains tested in LB media and induced at an OD_{600} of 0.5. Productivity was calculated over 48 h.

Strain	Max. Cell Density (g/L)	Max. Carotenoid Conc. (mg/L)	Max. Carotenoid Content (mg/g)	Time (h)	Productivity (µg/g·h)
1	2.67 ± 0.58	2.43 ± 0.86	1.07 ± 0.24	48	22.4 ± 5.0
2	2.17 ± 0.21	6.05 ± 0.95	3.27 ± 1.18	48	68.2 ± 24.6
3	1.57 ± 0.21	4.16 ± 1.86	2.87 ± 0.58	48	59.8 ± 12.1
4	1.90 ± 0.17	0.81 ± 0.16	0.65 ± 0.12	48	13.6 ± 2.5
5	1.73 ± 0.21	6.00 ± 0.47	4.19 ± 0.38	48	87.3 ± 7.9
6	1.47 ± 0.15	2.27 ± 0.27	1.59 ± 0.25	48	33.1 ± 5.2

Previous unpublished results have indicated that the IUP strains, when grown with a lycopene-producing plasmid, p5T7-lycipi-ggpps, outperform the trcMEP pathway. However, these strains were grown in M9 media. Therefore, a third experiment was conducted culturing these strains in M9 media. Furthermore, LB media could possibly increase the total carotenoid concentrations as there is some carotenoids present in yeast extract (Gupta, Jha, Pal, & Venkateshwarlu, 2007). Additionally, a third plasmid system was created plasmids containing p5T7-lycipi-IspA and pACT7-astaipi, which were paired with the native MEP, trcMEP, and pSEVA228-pro4IUP to create strains 7, 8 and 9. This added *IspA* to the plasmids since the bottlenecks in carotenoid production in *E. coli* were previously identified: the conversion of FPP to GGPP, which was improved by the change from *crtE* to *ggpps*, followed by production of FPP (*IspA*) (Yang & Guo, 2014). The results are presented in **Fig. 12.** Growth of all of the cultures in M9 media was lower than in LB, which was expected as there is only a limited amount of glucose available (**Fig. 12A**). However, unlike in LB media, there was no decrease in growth of the trcMEP or IUP containing strains**.** When the MEP pathway was upregulated and the strains were grown in M9 media, the pAC-BETAipi/pCBFD1 strain (**Fig 13C** – Strain 2) experienced a 1.4-fold increase in carotenoid content, and the p5T7-astaipi-ggpps strain (**Fig 13C** – Strain 5) experienced a 4.1-fold increase, to a content of 1.17 ± 0.08 mg/g dcw, however this was lower than the previous LB experiments.

Interestingly, in M9 media, the IUP strains showed much larger increases in carotenoid production. Strain 3, containing pAC-BETAipi and pCBFD1, had the highest increase in concentration, producing 11.3 mg/L of carotenoids and showed a 13.1-fold increase in carotenoid content compared to the wild-type strain with a content of 9.43 ± 2.21 mg/g dcw, as shown in **Fig. 12B &**

C. In all cases, in M9 media, the IUP strains performed better than all other upstream isoprenoid pathways.

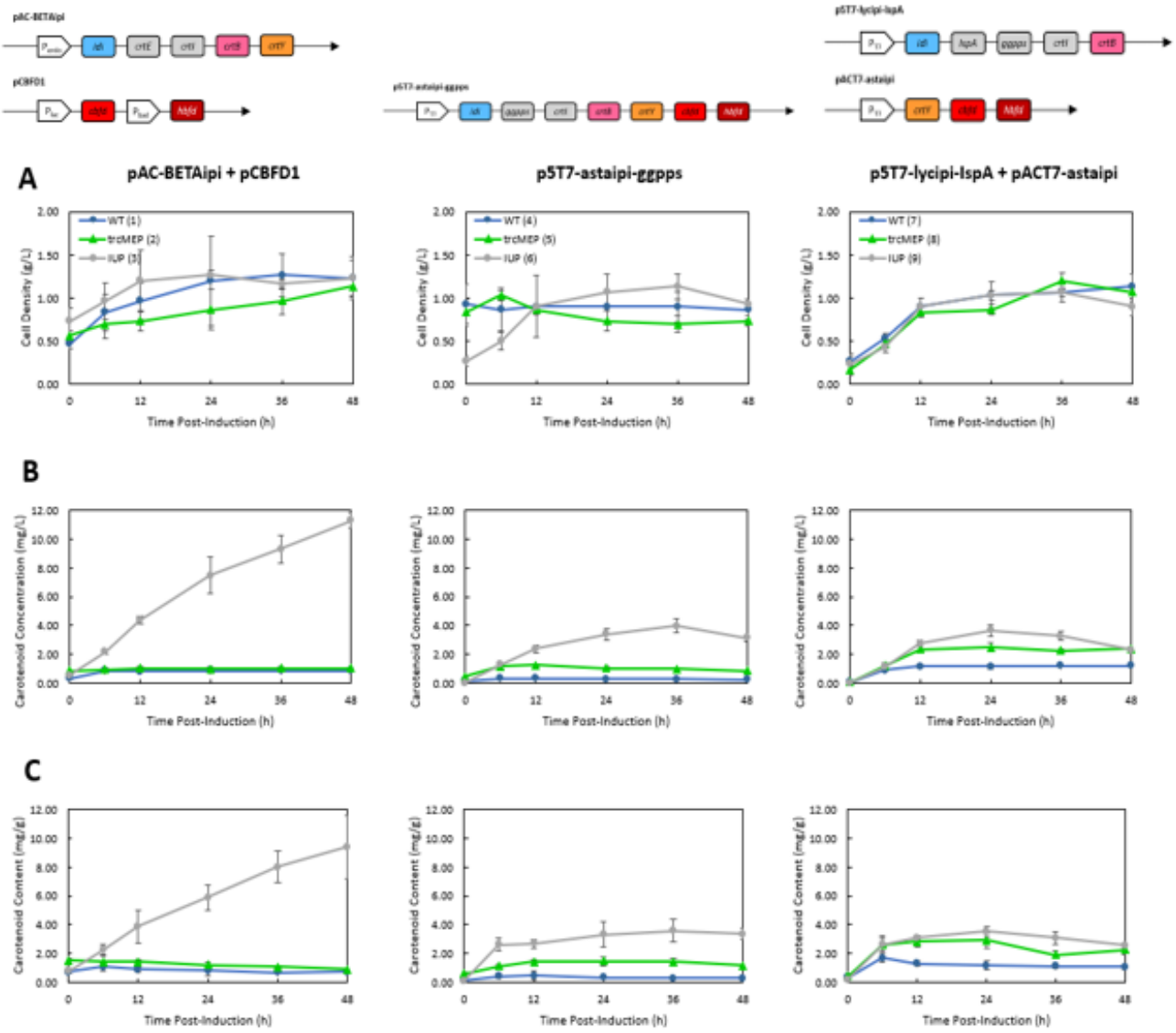

Fig. 12 – Culture performance for each of the nine carotenoid-producing strains of *E. coli* in M9 media. **A**: Growth profiles, **B:** total carotenoid concentration, **C**: total carotenoid content.

The productivity of each strain was also calculated over the 48-hour growth period, based on the maximum recorded carotenoid content (**Table 7)**. Using M9 media resulted in the highest productivity for the IUP strains, which coincides with an increase in total carotenoid concentration, particularly for Strain 3. For the trcMEP strains, productivity was higher in LB media than in M9 media.

Table 7 – Total carotenoids and productivity of each cell plasmid system in M9 media. Productivity is calculated over 48 h.

Strain	Max. Cell Density (g/L)	Max. Carotenoid Conc. (mg/L)	Max. Carotenoid Content (mg/g)	Time (h)	Productivity (µg/g·h)
1	1.27 ± 0.25	0.87 ± 0.05	1.08 ± 0.26	48	22.5 ± 5.4
2	1.13 ± 0.12	1.04 ± 0.07	1.44 ± 0.15	48	31.3 ± 3.3
3	1.27 ± 0.06	11.32 ± 0.50	9.43 ± 2.21	48	196.4 ± 46.0
4	0.93 ± 0.23	0.34 ± 0.05	0.46 ± 0.30	48	9.5 ± 6.2
5	1.03 ± 0.06	1.23 ± 0.07	1.46 ± 0.31	48	30.4 ± 6.4
6	1.13 ± 0.15	3.98 ± 0.46	3.58 ± 0.79	48	74.6 ± 16.5
7	1.13 ± 0.15	1.19 ± 0.01	1.71 ± 0.34	48	35.5 ± 7.1
8	1.20 ± 0.10	2.49 ± 0.33	2.90 ± 0.54	48	60.4 ± 11.2
9	1.07 ± 0.06	3.65 ± 0.39	3.53 ± 0.36	48	73.6 ± 7.5

Based on the results from these three studies, some notable trends were present. It was clear that the inclusion of the IUP pathway had a positive effect on carotenoid production when compared to the wild-type strains. However, when using LB media, the upregulation of the MEP pathway had an even greater effect. One possible explanation for this observation is that the MEP pathway requires more proteins and uses pyruvate and G3P from central carbon metabolism as its substrates. Considering that LB media is very rich in nutrients, which results in a faster growth rate, the MEP pathway outperforms the IUP pathway under these conditions. However, under the more restrictive growth conditions of M9 media, the IUP pathway outperformed the trcMEP strains. This is consequential since it would be much more economically desirable to use a cheaper media such as M9 than a complex media like LB in large-scale production plants (J. Gao et al., 2013).

Other possible effects on carotenoid production include the number of plasmids in each system, although low copy number plasmids were used, and there are differences in promoter strengths and number of promoters for each system. Both the p5T7-lycipi-IspA and pACT7-astaipi plasmids are induced with IPTG. Therefore, the effective concentration of IPTG dissolved in the media is halved when two T7 promoters are present. Furthermore, in nearly all the experiments, the carotenoid concentration of the pAC-BETAipi/pCBFD1 strains were higher than those of the

equivalent p5T7-astaipi-ggpps strains. Since these plasmids use a combination of inducible and constitutive promoters, it may be worthwhile to perform a combinatorial study of promoters to optimize these strains for the best possible assembly.

A decrease in carotenoid concentration near the 36-hour or 48-hour time points was also observed in some of the strains. This may be a result of carotenoid degradation over time, or the leakage of carotenoids out of the cell and into the media as the cells become more saturated. The carotenoids released into the media were not recovered during the extraction procedure used, since the liquid phase is removed through centrifugation.

Finally, the enzymes used in each isoprenoid pathway and the carotenoid pathways are known to have different optimal temperatures (Chatzivasileiou et al., 2018; Cunningham & Gantt, 2011). The IUP pathway enzymes were found to have significantly higher flux at 37°C compared to 30°C (Chatzivasileiou et al., 2018). However, *crtY*, which forms β-carotene, is only functional until 32°C (Bhosale & Gadre, 2002). Thus, all experiments were conducted at 30°C. Furthermore, in previous studies, lycopene productivity was significantly higher than seen in this work, with strains reaching a lycopene content of 8.53 mg/g dcw in only 5 h compared to 48 h in this work (Chatzivasileiou et al., 2018). In order to better understand the effects of the promoters and growth temperature on carotenoid productivity, two additional experiments were performed.

4.2 Effect of Temperature and IPTG Concentration on Carotenoid Production

To better understand the effect of temperature on the IUP pathway, the plasmid p5T7-lycipi-ggpps, which acted as the template for p5T7-astaipi-ggpps and p5T7-lycipi-IspA, and pSEVA228-pro4IUP were transformed into MG1655 (DE3) and these strains were cultures in M9 media at either 30 or 37°C. The results are presented in **Fig. 13**.

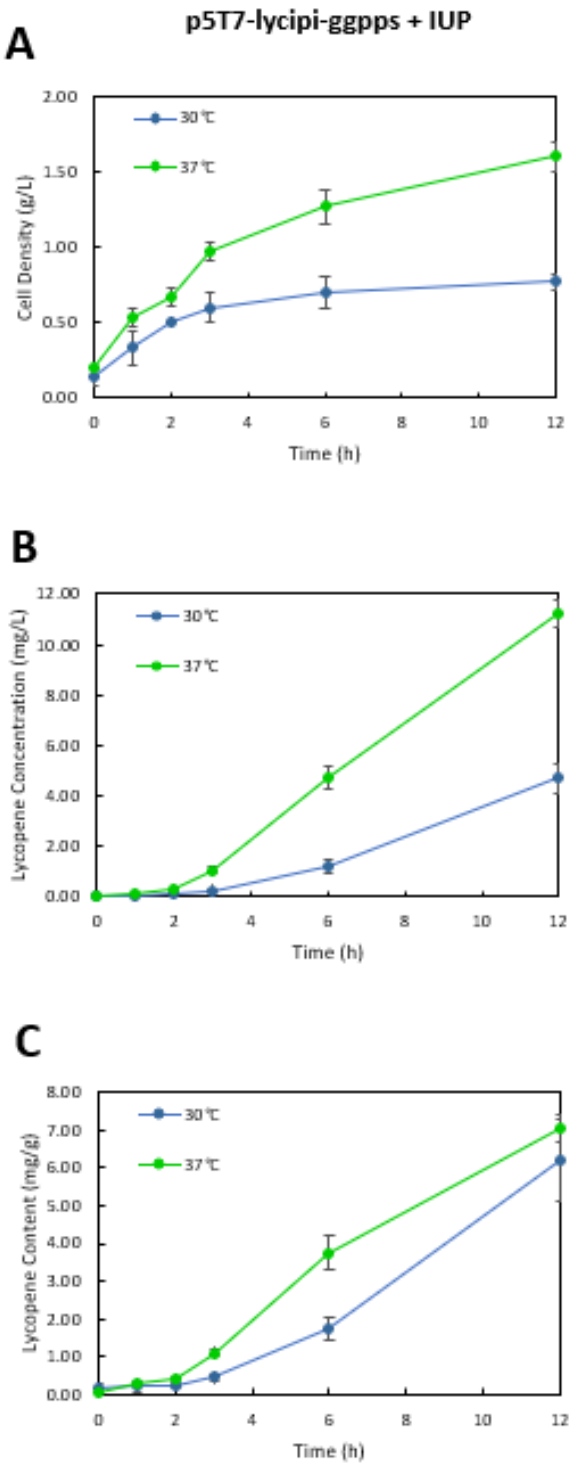

Fig. 13 – Lycopene production using p5T7-lycipi-ggpps and the IUP pathway at two different temperatures. **A:** Cell growth curves. **B:** Carotenoid concentration profiles. **C:** Carotenoid content profiles.

Growth of the strains was significantly improved at 37°C resulting in higher maximum cell density. Additionally, lycopene concentration and lycopene content in the cells was also significantly higher in the 37°C cultures confirming that temperature affects the IUP pathway flux and subsequently the flux of the carotenoid pathway. As a result, it would be prudent to search for homologs of *crtY, cbfd, hbfd, ck,* and *ipk* which have similar optimal temperatures, ideally at 37°C.

As it was surprising that the pAC-BETAipi/pCBFD1 plasmid system, which contains a constitutive endogenous promoter, a lac promoter, and an arabinose-inducible promoter, outperformed the p5T7-astaipi-ggpps system which has a stronger T7 promoter, an experiment was carried out to investigate the effect of IPTG concentration on carotenoid production. Strain 6, containing p5T7-astaipi-ggpps and pSEVA228-pro4IUP, was induced with IPTG concentrations ranging from 0 mM to 1.0 mM. It was found that IPTG concentration does have a significant positive effect on carotenoid concentration. Since carotenoid concentration continued to increase after 48 h, the experiments were continued up to 72 hours, shown in **Fig. 14**.

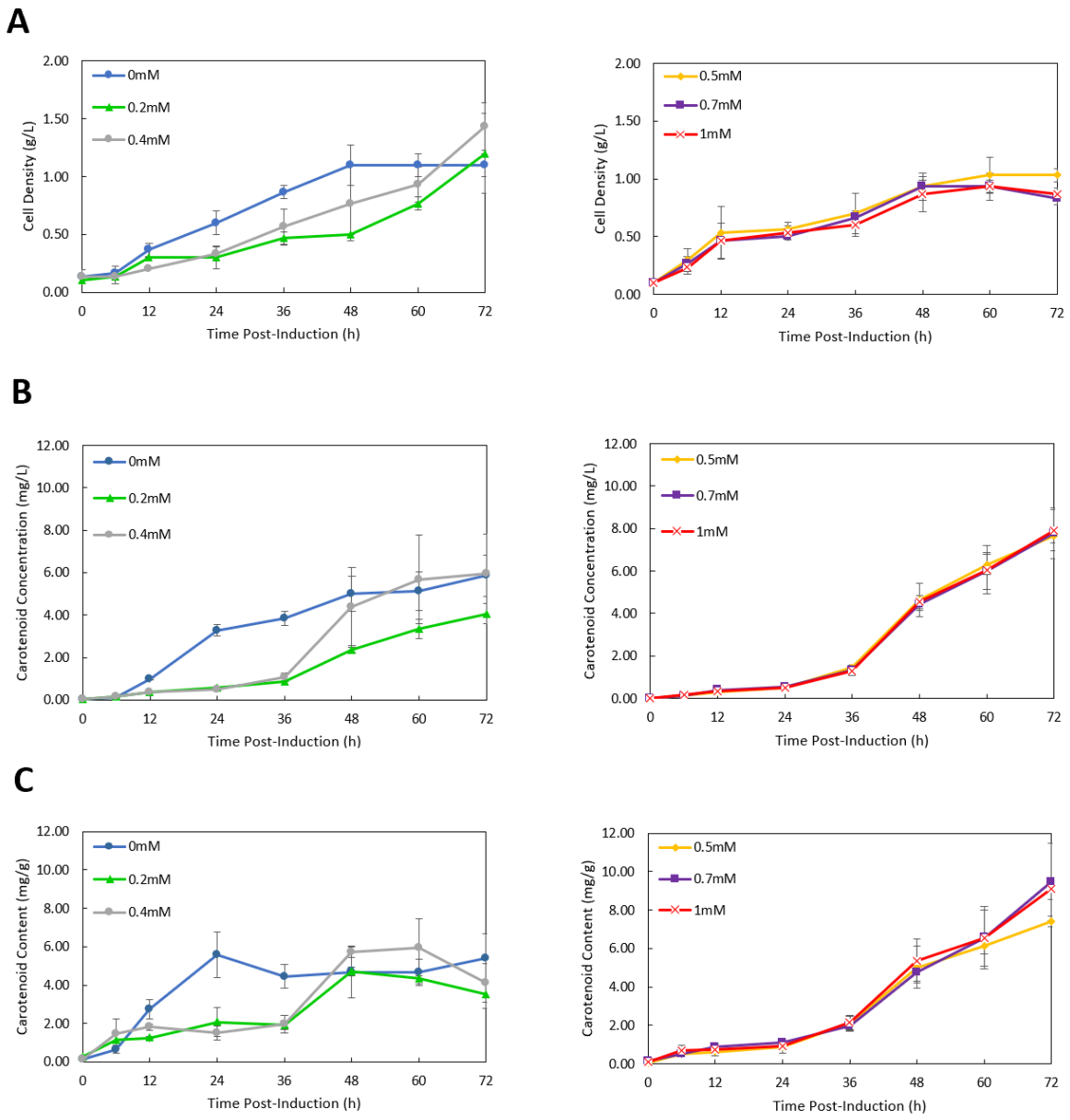

Fig. 14 – Concentration profiles for Strain 6 when altering IPTG concentration. **A:** Cell growth curves for each case. **B:** Carotenoid concentration profiles for each case. **C:** Carotenoid content profiles.

The highest recorded concentration occurred with an IPTG concentration of 0.7 mM, as shown in **Fig. 15**. When IPTG concentration was optimized, the carotenoid production in the IUP strain 6 containing p5T7-astaipi-ggpps was identical to the production in the IUP Strain 3 containing pAC-BETAipi/pCBFD1, 9.44 ± 2.01 mg/g dcw vs. 9.43 ± 2.21 mg/g dcw, respectively. However, IPTG levels this high negatively influenced the final cell density. In the trials with IPTG concentrations of 0.5 mM and higher, the maximum recorded cell dry weight decreased. As a result, for future experiments, it would be prudent to not exceed an IPTG concentration of 0.5 mM, which yielded a concentration of 7.40 ± 0.26 mg/g, given the drawbacks of excess IPTG in the culture media.

Unexpectedly, the controls containing no IPTG also produced similar amounts of carotenoids as the 0.2 mM and 0.4 mM induction cultures. This may be due to the inherent strength of the T7 promoter without the metabolic burden of IPTG, or to leaky expression, as this system uses *lacI* rather than the more tightly regulated *lacI*^{q} repressor (Sellitti, Pavco, & Steege, 1987).

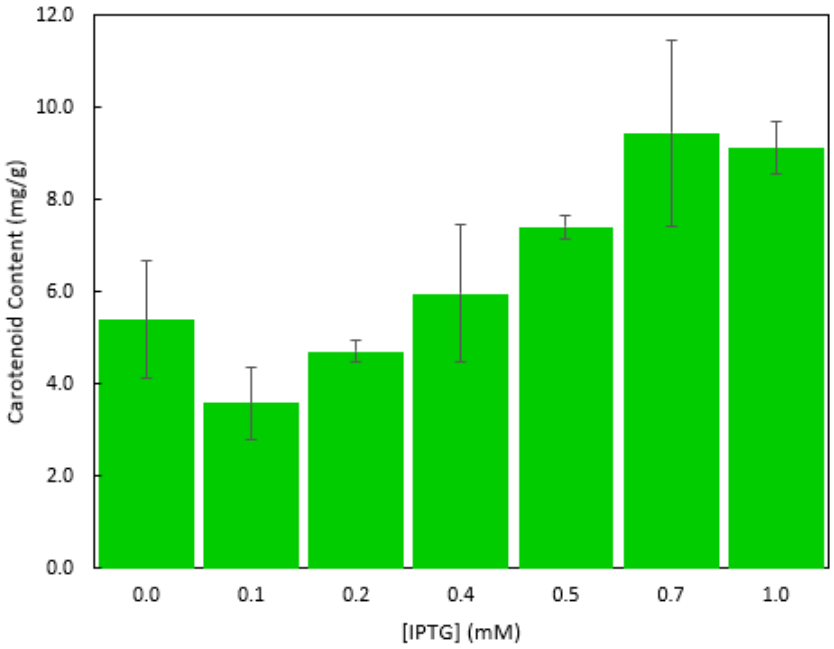

Fig. 15 – Effect of IPTG concentration on the maximum carotenoid content in Strain 6. The displayed values were obtained from the time point that recorded the highest carotenoid content, after inducing the system with IPTG. The carotenoid content at 0.1mM IPTG was retrieved from the experiment in **Fig. 12**.

4.3 Effect of Adding Casamino Acids

Finally, one major difference between M9 media and LB media is the lack of amino acids or peptides available for protein synthesis. In order to investigate the effect of adding amino acids on carotenoid production, Strain 6 was cultivated in M9 supplemented with 5 g/L casamino acids. Casamino acids act as an additional nutrient source and a source of amino acids for protein synthesis, which could increase the metabolic rate of the cell. However, it was found that when compared to the experiments preformed previously, there was no significant difference in the carotenoid production with and without casamino acids as shown in **Fig. 16**. However, since more time points were recorded within the first six hours of this experiment, this study gave a more accurate illustration of the productivity of the system, which was shown to be highest between the time points of 3 h and 6 h.

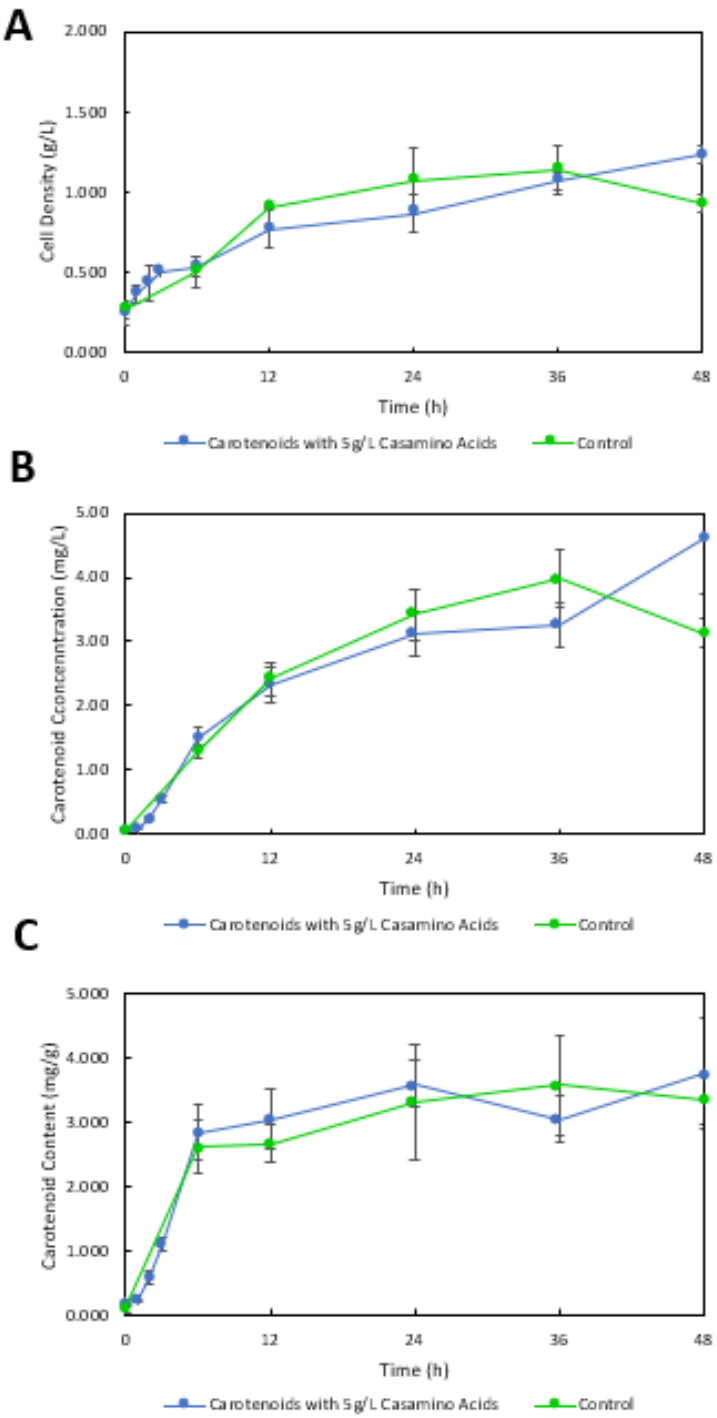

Fig. 16 – Effect of supplementing M9 media with 5 g/L casamino acids on carotenoid content in Strain 6. The control experiment is derived from the experiments given in **Fig. 12. A:** Cell growth curves. **B:** Carotenoid concentration profiles. **C:** Carotenoid content profiles.

4.4 HPLC Analysis

UV spectroscopy is often used for simple measurements of total carotenoids which all absorb light between 450-500 nm (Chen & Wei, 2017). However, strains capable of producing carotenoids after lycopene will likely contain a mixture of carotenoids rather than one pure carotenoid. In order to determine the purity of astaxanthin in these carotenoid producing strains, carotenoids must be separated and quantified using high pressure liquid chromatography (HPLC). The carotenoid compositions of the most productive strains, 3, 6 and 9, were analyzed. Strains were grown in triplicate in M9 media and carotenoids were extracted after 48 h post-induction. Representative chromatograms from the HPLC analysis are shown in **Fig. C 2**, and the compositions are summarized in **Table 8**.

Table 8 – Carotenoid composition of strains 3, 6 and 9. Purified standards were used to confirm the identity of each peak (n=3 ± 1σ).

	Concentration in mg/L (% Purity)		
Compound	**Strain 3**	**Strain 6**	**Strain 9**
Astaxanthin/ Zeaxanthin^	*n.d.	0.84 ± 0.07 (23.1 ± 0.78)	0.95 ± 0.11 (36.0 ± 2.45)
Canthaxanthin	n.d.	0.86 ± 0.07 (23.7 ± 0.81)	0.14 ± 0.12 (5.0 ± 4.30)
β-Carotene	13.85 ± 1.14 (99.7 ± 0.41)	1.64 ± 0.05 (45.3 ± 1.87)	0.54 ± 0.07 (20.2 ± 0.32)
Lycopene	n.d.	n.d.	1.03 ± 0.10 (38.8 ± 2.35)
Unknown	0.03 ± 0.06 (0.24 ± 0.41)	0.28 ± 0.03 (7.8 ± 0.31)	n.d.

^ These peaks could not be resolved using the current method
*n.d. = not detectable

Unfortunately, we were not able to resolve the astaxanthin and zeaxanthin peaks which co-eluted at 2.7 min. Each strain produced a significant amount of β-carotene, as is evident from the peaks at 4 min where the β-carotene standard eluted, shown in **Fig. C 2**. Surprisingly, Strain 3 contained nearly 100% β-carotene, which is not consistent with other work using this plasmid system (Cunningham & Gantt, 2011). This may be due to the *lacI* repressor present in *E. coli* MG1655 acting on the lac promoter on pCBFD1 prevents the expression of *hbfd*. However, cultures containing these plasmids used the XL1-Blue host background, which contains the $lacI^q$ repressor (Agilent Technlogies, n.d.) and were not induced with IPTG in other reports (Cunningham & Gantt, 2011). Upon further analysis, the promoter region does appear to contain the *lac* operator

sequence. This would effectively prevent the formation of astaxanthin. However, no canthaxanthin was formed either which is the product of *cbfd* which was induced with arabinose. This may be as a result of lack of induction and adding IPTG may be necessary. On the other hand, Strains 6 and 9 both yielded astaxanthin and/or zeaxanthin, which is indicated by a peak at 2.7 min. Interestingly, Strain 6 showed a peak at 3.39 min that did not match any of the carotenoid standards. This may be an isomer of canthaxanthin since the peaks are situated close to one another. Additionally, Strain 9 showed a strong peak of lycopene at 13.67 min, which was calculated to be 38.8 ± 2.35% of the total carotenoid concentration. The high lycopene concentration may be due to a combination of the lower level of induction, since both p5T7-lycipi-IspA and pACT7-astaipi are induced with IPTG, and the addition of *IspA* to this system. It is clear from this work that the order and promoters used in operon construction is critical for astaxanthin production and that changes in protein expression level and cellular concentration of proteins likely had an affect on the overall purity of astaxanthin in these strains. This could be further investigated by analysing the protein concentrations in each strain using LC-MS and comparing to the levels of each carotenoid. Finally, one major issue across all the analyses was that the astaxanthin and zeaxanthin standards had the same residence time, making them impossible to differentiate. This was resolved by changing the mobile phase. Additionally, to address the potential lack of induction in Strain 3, 0.1 mM IPTG was added to the new cell culture. The results from the change in experimental procedure are given in **Table 9**.

Table 9 – Carotenoid composition of Strains 3, 6 and 9 using the new HPLC method. Purified standards were used to confirm the identity of each peak (n=3 ± 1σ).

	Concentration in mg/L (% Purity)		
Compound	**Strain 3**	**Strain 6**	**Strain 9**
Astaxanthin	0.11 ± 0.05 (7.45 ± 3.02)	0.49 ± 0.02 (42.21 ± 1.68)	0.59 ± 0.00 (63.08 ± 0.36)
Zeaxanthin	0.13 ± 0.07 (8.13 ± 4.62)	0.15 ± 0.01 (12.89 ± 1.28)	0.18 ± 0.01 (19.69 ± 0.74)
Canthaxanthin	*n.d.	0.12 ± 0.02 (10.35 ± 1.59)	n.d.
β-Carotene	0.94 ± 0.12 (60.17 ± 7.49)	0.40 ± 0.01 (34.85 ± 1.59)	0.15 ± 0.00 (16.39 ± 0.44)
Unknown	0.28 ± 0.03 (18.02 ± 1.99)	n.d.	n.d.

*n.d. = not detectable

Using the new method, we were able to separately resolve astaxanthin and zeaxanthin, which eluted at 8.4 min and 9.4 min, as seen in **Fig. C 3**. Strain 3 showed a positive response to IPTG induction, as the astaxanthin content increased to 7.45 ± 3.02%, and an increase in zeaxanthin concentration was also detected. However, an unknown peak was detected at 13.7 min, which was close to the β-carotene peak, which eluted at 15.2 min. This may be an isomer of β-carotene, and so the β-carotene calibration was used to determine its concentration. While the culture conditions of Strains 6 and 9 were unchanged, there was still a change in carotenoid composition. The astaxanthin content of both strains nearly doubled, increasing to 42.21 ± 1.68% in Strain 6 and 63.08 ± 0.36% in Strain 9. The unknown peak initially present with Strain 6 was also not detected. Interestingly, Strain 9, which originally had a strong lycopene concentration, did not contain any lycopene or canthaxanthin in the second trial. Another experimental trial would need to be performed to assess the repeatability of the experiment, since the compositions of the strains were so different between the two trials, especially with Strain 9. It may also be worthwhile, when considering operon construction, to use a different inducer for the second operon in the system since they may be competing for IPTG.

5 Conclusions and Recommendations

Overall, astaxanthin production was successfully incorporated into wild-type and trcMEP *E. coli* strains. Inclusion of the isopentenol utilization pathway was confirmed to significantly increase carotenoid production and productivity, and cultivation of these strains in M9 media had the greatest productivities. IPTG concentration had a significant effect on overall carotenoid production but at high concentrations, inhibited cell growth. The IUP was also shown to have increased flux at higher temperatures accounting for some of the decreased flux compared to previous work. However, the HPLC results showed a large accumulation of β-carotene in addition to astaxanthin, shedding light on the importance of operon construction on astaxanthin production. Furthermore, HPLC results were not reproducible, therefore these experiments must be repeated before a more rational approach to operon construction can be taken.

There are a number of possible avenues to pursue to increase the productivity of the developed strains. First, a combinatorial study of promoter combinations would be useful for optimizing the level of enzyme expression in the carotenoid pathways. This could be compared to the intracellular concentrations of each enzyme in the different strains and compared to astaxanthin purity. Secondly, in order to make a fair comparison of the trcMEP to the IUP pathways, the IUP pathway should also be inserted into the genome of MG1655 (DE3) rather than housed on a plasmid. This would eliminate the need for pSEVA228-pro4IUP and its antibiotic marker reducing the metabolic burden on the cell.

References

Agilent Technlogies. (n.d.). XL1-Blue Competent Cells, Manual Catalog #200249, 10–11. Retrieved from http://www.chem-agilent.com/pdf/strata/200249.pdf

Ajikumar, P. K., Xiao, W. H., Tyo, K. E. J., Wang, Y., Simeon, F., Leonard, E., … Stephanopoulos, G. (2010). Isoprenoid pathway optimization for Taxol precursor overproduction in Escherichia coli. *Science*, *330*(6000), 70–74. https://doi.org/10.1126/science.1191652

Alonso-Gutierrez, J., Chan, R., Batth, T. S., Adams, P. D., Keasling, J. D., Petzold, C. J., & Lee, T. S. (2013). Metabolic engineering of Escherichia coli for limonene and perillyl alcohol production. *Metabolic Engineering*, *19*, 33–41. https://doi.org/10.1016/j.ymben.2013.05.004

Ambati, R. R., Phang, S. M., Ravi, S., & Aswathanarayana, R. G. (2014a). Astaxanthin: Sources, Extraction, Stability, Biological Activities and Its Commercial Applications—A Review, 128–152. https://doi.org/10.3390/md12010128

Ambati, R. R., Phang, S. M., Ravi, S., & Aswathanarayana, R. G. (2014b). Astaxanthin: Sources, Extraction, Stability, Biological Activities and Its Commercial Applications—A Review. *Marine Drugs*, 128–152. https://doi.org/10.3390/md12010128

Barredo, J., García-Estrada, C., Kosalkova, K., & Barreiro, C. (2017). Biosynthesis of Astaxanthin as a Main Carotenoid in the Heterobasidiomycetous Yeast Xanthophyllomyces dendrorhous. *Journal of Fungi*, *3*(3), 44. https://doi.org/10.3390/jof3030044

Batghare, A. H., Singh, N., & Moholkar, V. S. (2018). Investigations in ultrasound – induced enhancement of astaxanthin production by wild strain Phaffia rhodozyma MTCC 7536. *Bioresource Technology*, *254*(January), 166–173. https://doi.org/10.1016/j.biortech.2018.01.073

Bauer, A., & Minceva, M. (2019). Direct extraction of astaxanthin from the microalgae: Haematococcus pluvialis using liquid-liquid chromatography. *RSC Advances*, *9*(40), 22779–22789. https://doi.org/10.1039/c9ra03263k

Bhosale, P., & Gadre, R. V. (2002). Manipulation of temperature and illumination conditions for enhanced β-carotene production by mutant 32 of Rhodotorula glutinis. *Letters in Applied*

Microbiology, *34*(5), 349–353. https://doi.org/10.1046/j.1472-765X.2002.01095.x

Boussiba, S. (2000). Carotenogenesis in the green alga Haematococcus pluvialis : Cellular physiology and stress response, (Ii), 111–117.

Breitenbach, J., Misawa, N., Kajiwara, S., & Sandmann, G. (1996). Expression in Escherichia coli and properties of the carotene ketolase from Haematococcus pluvialis. *FEMS Microbiology Letters*, *140*(2–3), 241–246. https://doi.org/10.1016/0378-1097(96)00187-5

Capelli, B., Bagchi, D., & Cysewski, G. R. (2013). Synthetic astaxanthin is significantly inferior to algal-based astaxanthin as an antioxidant and may not be suitable as a human nutraceutical supplement. *Nutrafoods*, *12*(4), 145–152. https://doi.org/10.1007/s13749-013-0051-5

Chatzivasileiou, A. O., Ward, V., Edgar, S., & Stephanopoulos, G. (2018). A novel two-step pathway for isoprenoid synthesis. *PNAS*, *n.a*(2), 506–511. https://doi.org/10.1073/pnas.1812935116

Chen, J., & Wei, D. (2017). Rapid Estimation of Astaxanthin and the Carotenoid-to-Chlorophyll Ratio in the Green Microalga Chromochloris zofingiensis Using Flow Cytometry, 1–23. https://doi.org/10.3390/md15070231

Chou, Y., Ko, C., Yen, C., Chen, L. O., & Shaw, J. (2019). Multiple promoters driving the expression of astaxanthin biosynthesis genes can enhance free-form astaxanthin production. *Journal of Microbiological Methods*, *160*(March), 20–28. https://doi.org/10.1016/j.mimet.2019.03.012

Cunningham, F. X., & Gantt, E. (2011). Elucidation of the Pathway to Astaxanthin in the Flowers of Adonis aestivalis . *The Plant Cell*, *23*(8), 3055–3069. https://doi.org/10.1105/tpc.111.086827

Fradkov, A. F., Verkhusha, V. V., Staroverov, D. B., Bulina, M. E., Yanushevich, Y. G., Martynov, V. I., … Lukyanov, K. A. (2002). Far-red fluorescent tag for protein labelling. *Biochemical Journal*, *368*(1), 17–21. https://doi.org/10.1042/BJ20021191

Gao, J., Atiyeh, H. K., Phillips, J. R., Wilkins, M. R., & Huhnke, R. L. (2013). Development of low cost medium for ethanol production from syngas by Clostridium ragsdalei. *Bioresource Technology*, *147*, 508–515. https://doi.org/10.1016/j.biortech.2013.08.075

Gao, Z., Meng, C., Gao, H., Zhang, X., Xu, D., Su, Y., … Ye, N. (2013). Analysis of mRNA expression profi les of carotenogenesis and astaxanthin production of Haematococcus pluvialis under exogenous, 201–206.

Gupta, S. K., Jha, A. K., Pal, A. K., & Venkateshwarlu, G. (2007). Use of natural carotenoids for pigmentation in fishes. *Natural Product Radiance*, *6*(1), 46–49.

Henke, N. A., & Wendisch, V. F. (2019). Improved Astaxanthin Production with Corynebacterium glutamicum by Application of a Membrane Fusion Protein.

Jeong, T. H., Cho, Y. S., Choi, S., Kim, G., & Lim, H. K. (2018). Enhanced Production of Astaxanthin by Metabolically Engineered Non-mevalonate Pathway in Escherichia coli, *46*, 114–119.

Jiang, G. L., Zhou, L. Y., Wang, Y. T., & Zhu, M. J. (2017). Astaxanthin from Jerusalem artichoke: Production by fed-batch fermentation using Phaffia rhodozyma and application in cosmetics. *Process Biochemistry*, *63*(April), 16–25. https://doi.org/10.1016/j.procbio.2017.08.013

Jiang, G., Yang, Z., Wang, Y., Yao, M., Chen, Y., Xiao, W., & Yuan, Y. (2020). Enhanced astaxanthin production in yeast via combined mutagenesis and evolution. *Biochemical Engineering Journal*, *156*(January), 107519. https://doi.org/10.1016/j.bej.2020.107519

Kaewpintong, K., Shotipruk, A., & Powtongsook, S. (2007). Photoautotrophic high-density cultivation of vegetative cells of Haematococcus pluvialis in airlift bioreactor, *98*, 288–295.

Kirby, J., & Keasling, J. D. (2009). Biosynthesis of Plant Isoprenoids: Perspectives for Microbial Engineering. *Annual Review of Plant Biology*, *60*(1), 335–355. https://doi.org/10.1146/annurev.arplant.043008.091955

Krause, I. W., Paust, J., & Ernst, H. (1997). United States Patent 19, 4–8.

Li, Y., Lin, Z., Huang, C., Zhang, Y., & Wang, Z. (2015). Metabolic engineering of Escherichia coli using CRISPR – Cas9 meditated genome editing. *Metabolic Engineering*, *31*, 13–21. https://doi.org/10.1016/j.ymben.2015.06.006

Lin, Y., Lin, J., Wang, D., Chen, C., & Chiou, M. (2017). Safety assessment of astaxanthin derived from engineered Escherichia coli K-12 using a 13-week repeated dose oral toxicity study and

a prenatal developmental toxicity study in rats. *Regulatory Toxicology and Pharmacology*, *87*, 95–105. https://doi.org/10.1016/j.yrtph.2017.05.003

Lu, M., Zhang, Y., Zhao, C., Zhou, P., & Yu, L. (2010a). Analysis and Identifi cation of Astaxanthin and its Carotenoid Precursors from Xanthophyllomyces dendrorhous by High-Performance Liquid Chromatography, (2005).

Lu, M., Zhang, Y., Zhao, C., Zhou, P., & Yu, L. (2010b). Analysis and identification of astaxanthin and its carotenoid precursors from Xanthophyllomyces dendrorhous by high-performance liquid chromatography. *Zeitschrift Fur Naturforschung - Section C Journal of Biosciences*, *65 C*(7–8), 489–494. https://doi.org/10.1515/znc-2010-7-812

Lu, Q., Bu, Y. F., & Liu, J. Z. (2017). Metabolic engineering of Escherichia coli for producing astaxanthin as the predominant carotenoid. *Marine Drugs*, *15*(10). https://doi.org/10.3390/md15100296

Ma, T., Zhou, Y., Li, X., Zhu, F., Cheng, Y., Liu, Y., … Liu, T. (2016). Genome mining of astaxanthin biosynthetic genes from Sphingomonas sp. ATCC 55669 for heterologous overproduction in Escherichia coli. *Biotechnology Journal*, *11*(2), 228–237. https://doi.org/10.1002/biot.201400827

Matthews, P. D., & Wurtzel, E. T. (2000). Metabolic engineering of carotenoid accumulation in Escherichia coli by modulation of the isoprenoid precursor pool with expression of deoxyxylulose phosphate synthase. *Applied Microbiology and Biotechnology*, *53*(4), 396–400. https://doi.org/10.1007/s002530051632

Nogueira, M., Enfissi, E. M. A., Welsch, R., Beyer, P., Zurbriggen, M. D., & Fraser, P. D. (2019). Construction of a fusion enzyme for astaxanthin formation and its characterisation in microbial and plant hosts : A new tool for engineering ketocarotenoids. *Metabolic Engineering*, *52*(July 2018), 243–252. https://doi.org/10.1016/j.ymben.2018.12.006

Olaizola, M. (2000). Commercial production of astaxanthin from Haematococcus pluvialis using 25 , 000-liter outdoor photobioreactors, 499–506.

Panis, G., & Carreon, J. R. (2016). Commercial astaxanthin production derived by green alga Haematococcus pluvialis : A microalgae process model and a techno-economic assessment

all through production line. *ALGAL*, *18*, 175–190. https://doi.org/10.1016/j.algal.2016.06.007

Park, S. Y., Binkley, R. M., Kim, W. J., Lee, M. H., & Lee, S. Y. (2018). Metabolic engineering of Escherichia coli for high-level astaxanthin production with high productivity. *Metabolic Engineering*, *49*(August), 105–115. https://doi.org/10.1016/j.ymben.2018.08.002

Rad, S. A., Zahiri, H. S., Noghabi, K. A., Rajaei, S., Heidari, R., & Mojallali, L. (2012). Type 2 IDI performs better than type 1 for improving lycopene production in metabolically engineered E. coli strains. *World Journal of Microbiology and Biotechnology*, *28*(1), 313–321. https://doi.org/10.1007/s11274-011-0821-4

Ribeiro, L., Tramontin, R., Kildegaard, K. R., Sudarsan, S., & Borodina, I. (2019). Enhancement of Astaxanthin Biosynthesis in Oleaginous Yeast Yarrowia lipolytica via Microalgal Pathway.

Sellitti, M. A., Pavco, P. A., & Steege, D. A. (1987). lac repressor blocks in vivo transcription of lac control region DNA. *Proceedings of the National Academy of Sciences of the United States of America*, *84*(10), 3199–3203. https://doi.org/10.1073/pnas.84.10.3199

Shah, M. R., Liang, Y., Cheng, J. J., & Daroch, M. (2016). Astaxanthin-Producing Green Microalga Haematococcus pluvialis From Single Cell to High Value Commercial Products. *Plant Science*, *7*(April). https://doi.org/10.3389/fpls.2016.00531

Wang, Chia-wei, Oh, M., & Liao, J. C. (1999). Engineered Isoprenoid Pathway Enhances Astaxanthin Production in Escherichia coli.

Wang, Chonglong, Zada, B., Wei, G., & Kim, S. (2017). Metabolic engineering and synthetic biology approaches driving isoprenoid production in Escherichia coli. *Bioresource Technology*, *241*, 430–438. https://doi.org/10.1016/j.biortech.2017.05.168

Ward, V. C. A., Chatzivasileiou, A. O., & Stephanopoulos, G. (2018). Metabolic engineering of Escherichia coli for the production of isoprenoids. *FEMS Microbiology Letters*, *365*(10), 1–9. https://doi.org/10.1093/femsle/fny079

Wolfe, R. A., & Fowler, R. G. (1945). An Application of Spectrographic Methods to Chemical Concentrations of Trace Elements in Iron and Steel Analysis. *Journal of the Optical Society of America*, *35*(1), 86. https://doi.org/10.1364/josa.35.000086

Yang, J., & Guo, L. (2014). Biosynthesis of β-carotene in engineered E. coli using the MEP and MVA pathways. *Microbial Cell Factories*, *13*(1), 1–11. https://doi.org/10.1186/s12934-014-0160-x

Ye, L., Zhu, X., Wu, T., Wang, W., Zhao, D., Bi, C., & Zhang, X. (2018). Optimizing the localization of astaxanthin enzymes for improved productivity. *Biotechnology for Biofuels*, 1–9. https://doi.org/10.1186/s13068-018-1270-1

Yokoyama, A., Shizuri, Y., & Misawa, N. (1998). Production of New Carotenoids, Astaxanthin Glucosides, by Escherichia coli Transformants Carrying Carotenoid Biosynthetic Genes. *Tetrahedron Letters*, *39*, 3709–3712.

Yuan, L. Z., Rouvière, P. E., LaRossa, R. A., & Suh, W. (2006). Chromosomal promoter replacement of the isoprenoid pathway for enhancing carotenoid production in E. coli. *Metabolic Engineering*, *8*(1), 79–90. https://doi.org/10.1016/j.ymben.2005.08.005

Zhang, C., Seow, V. Y., Chen, X., & Too, H. P. (2018). Multidimensional heuristic process for high-yield production of astaxanthin and fragrance molecules in Escherichia coli. *Nature Communications*, *9*(1), 1–12. https://doi.org/10.1038/s41467-018-04211-x

Zhou, P., Xie, W., Li, A., Wang, F., Yao, Z., Bian, Q., … Ye, L. (2017). Alleviation of metabolic bottleneck by combinatorial engineering enhanced astaxanthin synthesis in Saccharomyces cerevisiae. *Enzyme and Microbial Technology*, *100*, 28–36. https://doi.org/10.1016/j.enzmictec.2017.02.006

Zhou, Y., Nambou, K., Wei, L., Cao, J., Imanaka, T., & Hua, Q. (2013). Lycopene production in recombinant strains of Escherichia coli is improved by knockout of the central carbon metabolism gene coding for glucose-6-phosphate dehydrogenase. *Biotechnology Letters*, *35*(12), 2137–2145. https://doi.org/10.1007/s10529-013-1317-0

Appendices

Appendix A: Plasmid Information

Table A 1 – List of the primers used for the plasmid assemblies. The plasmid pACT7-CBFD was made to act as an intermediate for the assembly of pACT7-astaipi, since there were many fragments to assemble.

Gene	Template	Assembly	Sequences
p5T7-lyc_bb	p5T7-lycipi-ggpps	p5T7-astaipi-ggpps	F: catgaatcaactcGCAGTACATAACGATGGAAC R: tcactccctgctTTGAACCCAAAAGGGCGG
crtY	pAC-BETAipi	p5T7-astaipi-ggpps	F: cttttgggttcaaAGCAGGGAGTGAGAGCGTATC R: cctcctgttagccAAAGCCTGCGCCAATCAC
cbfd	pCBFD1	p5T7-astaipi-ggpps	F: ggcgcaggctttGGCTAACAGGAGGAATTAAC R: ctttttctttctataggcgactcc*tc*TCGACGAATTCAGATCTGG
hbfd	pCBFD1	p5T7-astaipi-ggpps	F: GGAGTCGCCTATGAGAAAG R: gttatgtactgcGAGTTGATTCATGTAGATGATTGC
p5T7-lyc_bb (2)	p5T7-lycipi-ggpps	p5T7-lycipi-IspA	F: ataaaggatcACAGGAGTAGTGATGAATGAAG R: atatctccttTTGAACCCAAAAGGGCGG
IspA	p5T7-IspA-ads	p5T7-lycipi-IspA	F: ttgggttcaaAAGGAGATATACCATATGGACTTTC R: ctactcctgtGATCCTTTATTTATTACGCTGGATG
beta_bb	pAC-BETAipi	pACT7-CBFD	F: aacggcatgaGGCACCAATAACTGCCTTAAAAAAATTAC R: cgggcagtgaCATGAGACGCTGTGCCTTTAG
lacI_pT7	p5T7-lycipi-ggpps	pACT7-CBFD	F: gcgtctcatgTCACTGCCCGCTTTCCAG R: ctgttagcccCTACAGGGGAATTGTTATCCG
cbfd (2)	pCBFD1	pACT7-CBFD	F: tcccctgtagGGGCTAACAGGAGGAATTAAC R: gatatccaatTCGACGAATTCAGATCTGG
T7t	p5T7-lycipi-ggpps	pACT7-CBFD	F: aattcgtcgaATTGGATATCGGCCGGCC R: tattggtgccTCATGCCGTTTGTGATGG
CBFD_bb	pACT7-CBFD	pACT7-astaipi	F: tctacatgaaATTGGATATCGGCCGGCC R: actccctgctCCAATCTATTACTCTACTGCTTCATAATG
crtY (2)	pAC-BETAipi	pACT7-astaipi	F: aatagattggAGCAGGGAGTGAGAGCGTATC R: CACAACGGTTTTTTTCATCCTTTATC
hbfd (2)	pCBFD1	pACT7-astaipi	F: ggatgaaaaaaaccgttgtg*aa*GGAGTCGCCTATGAGAAAG R: gatatccaatTTCATGTAGATGATTGCGTTC

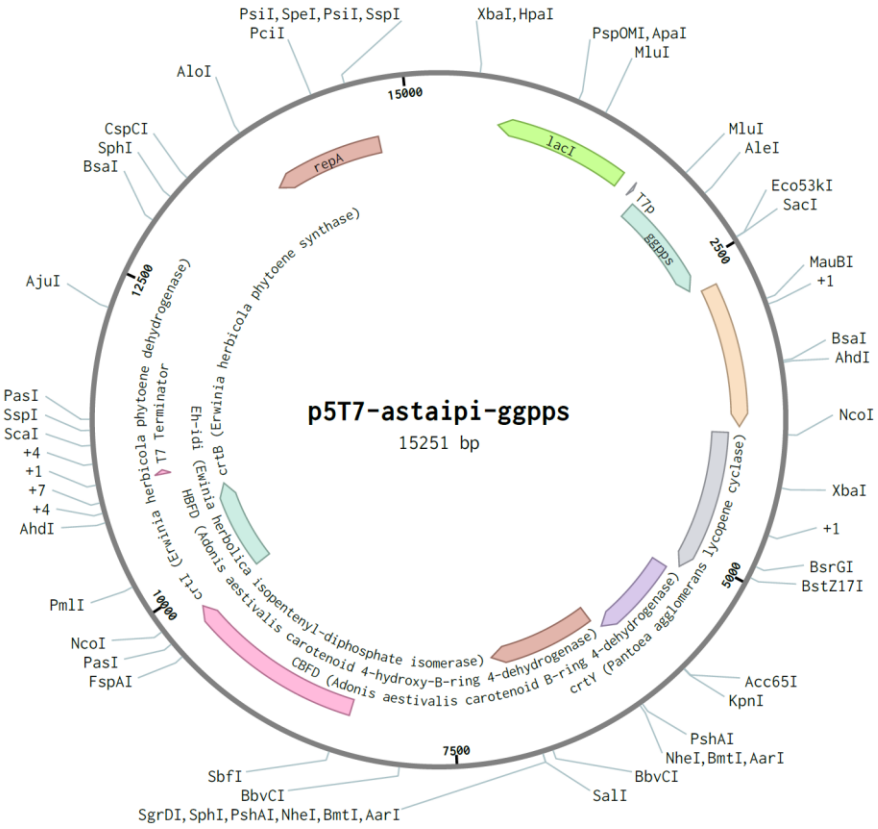

Fig. A 1 – Plasmid map of p5T7-astaipi-ggpps.

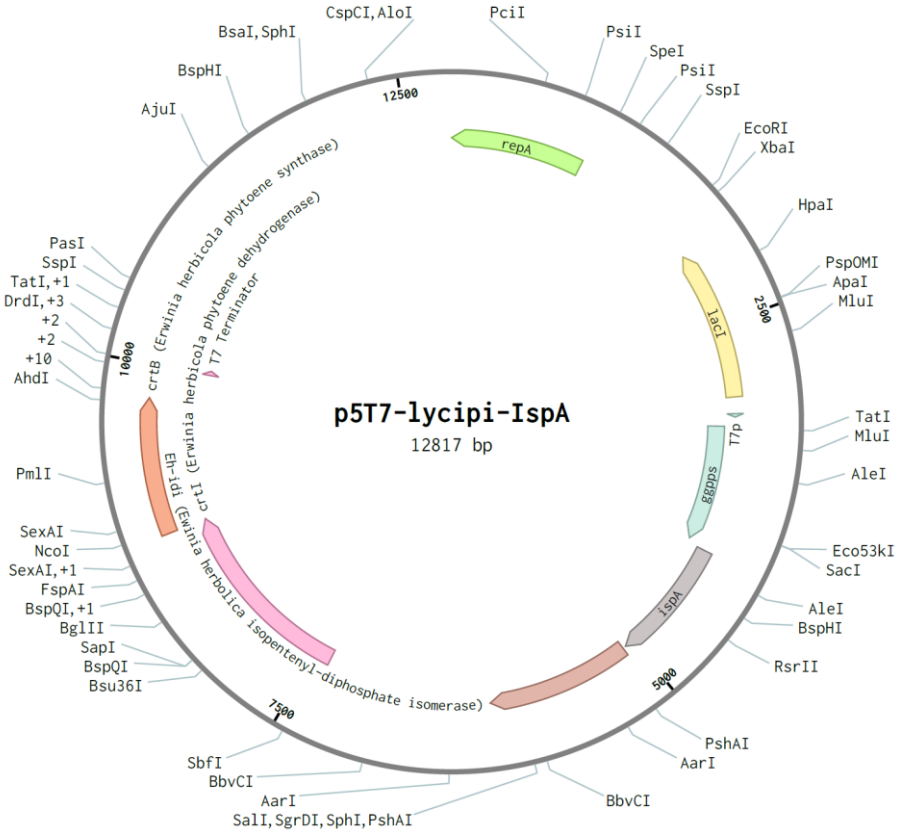

Fig. A 2 – Plasmid map of p5T7-lycipi-IspA. This plasmid works in conjunction with pACT7-astaipi.

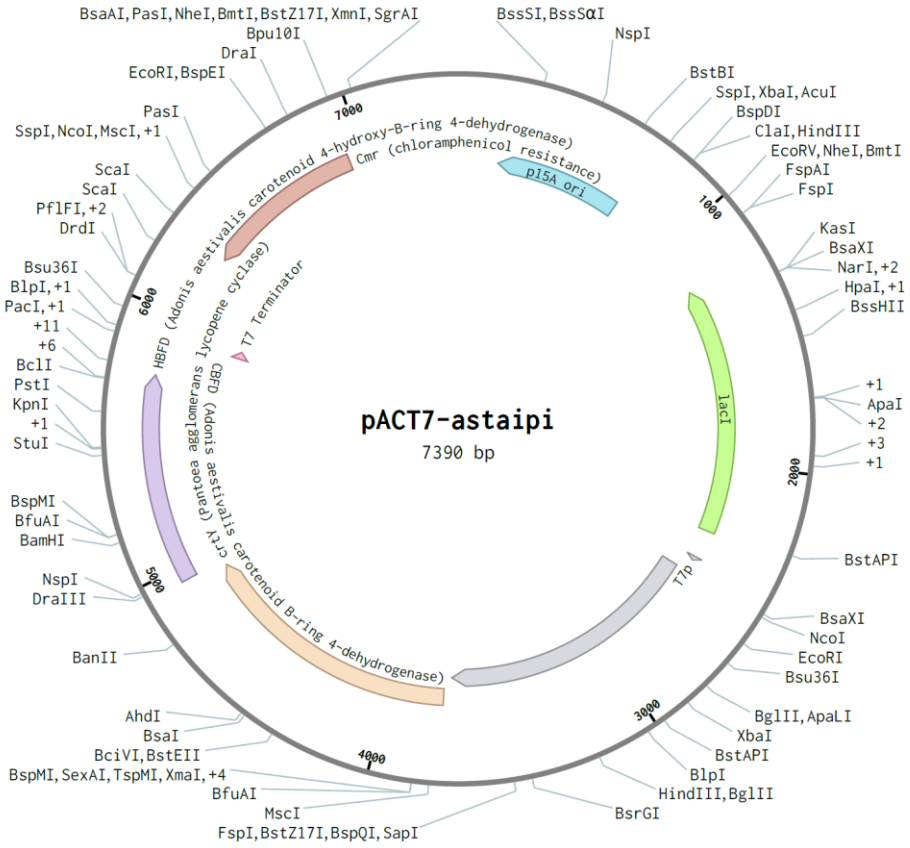

Fig. A 3 – Plasmid map of pACT7-astaipi. This plasmid works in conjunction with p5T7-lycipi-IspA.

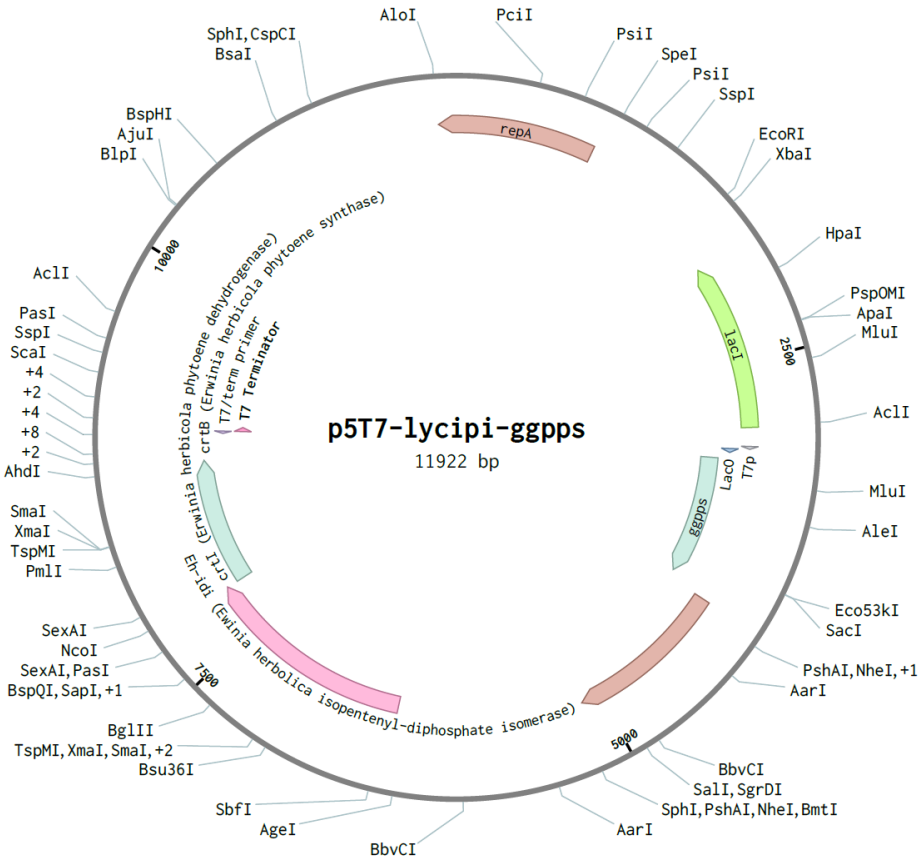

Fig. A 4 – Plasmid map of p5T7-lycipi-ggpps, which was used as the backbone for p5T7-astaipi-ggpps.

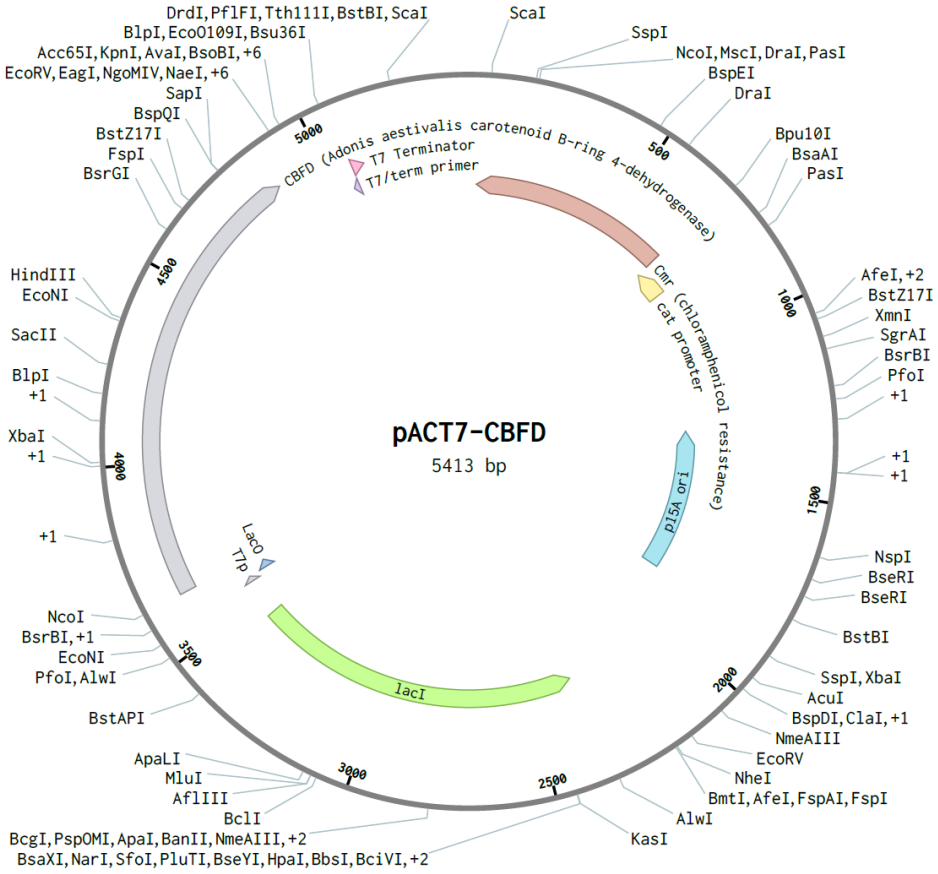

Fig. A 5 – Plasmid map of pACT7-CBFD, the intermediate plasmid for cloning pACT7-astaipi.

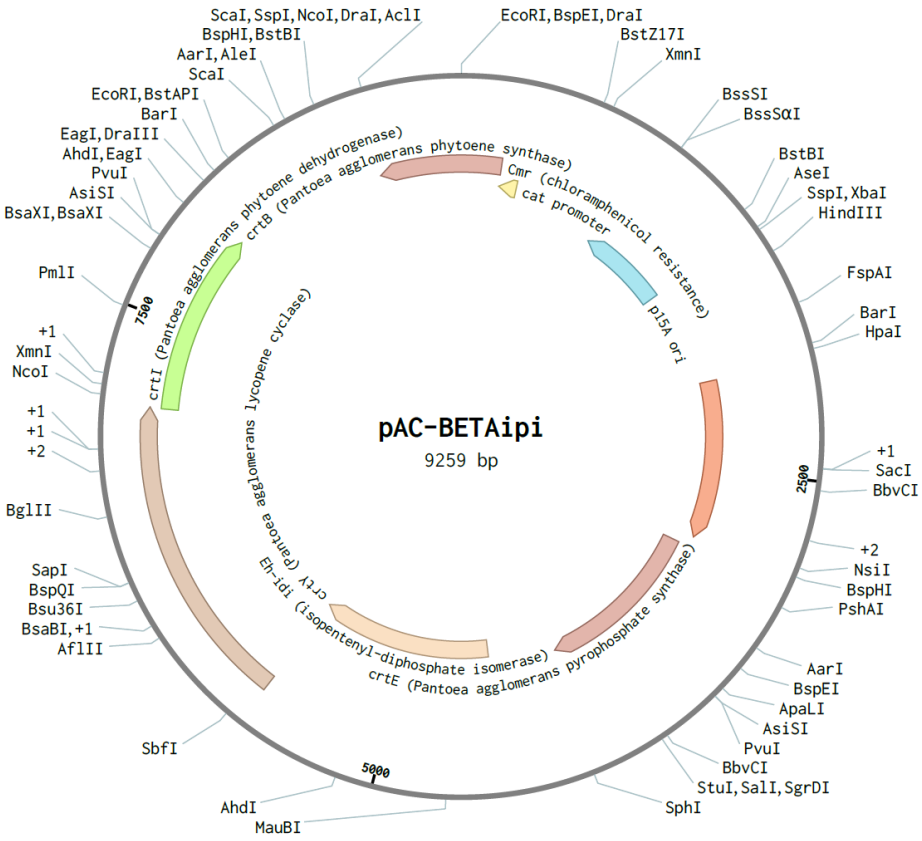

Fig. A 6 – Plasmid map of pAC-BETAipi, purchased from Addgene with pCBFD1.

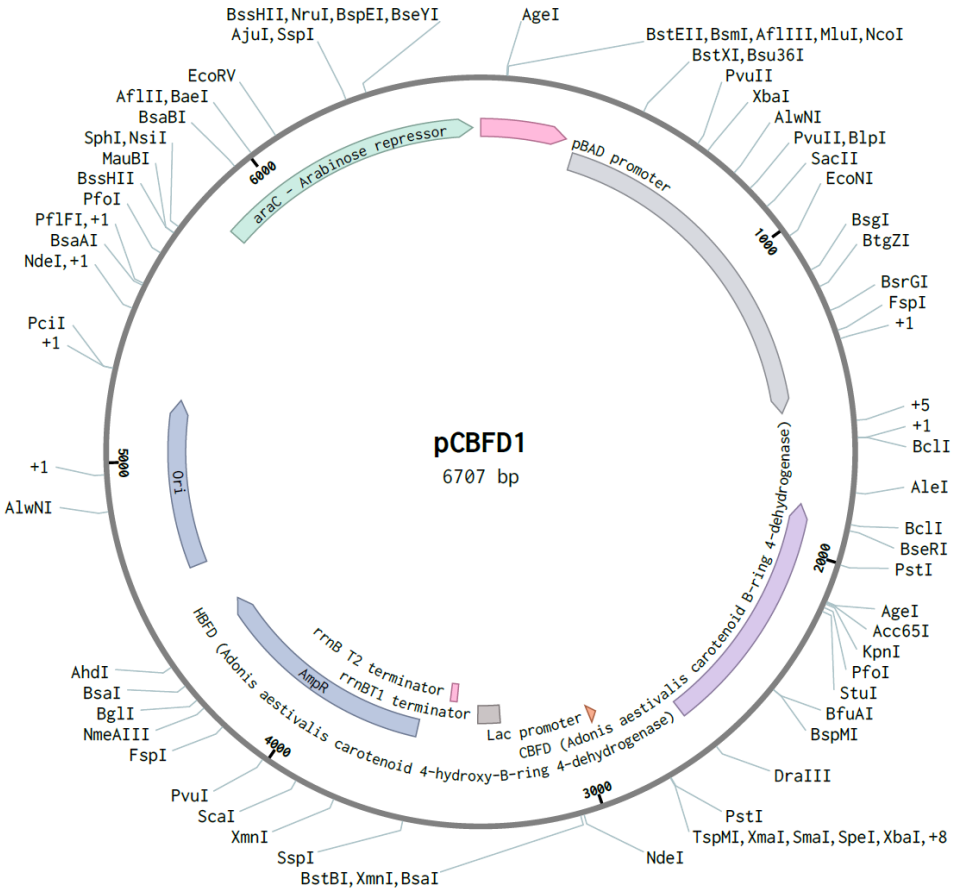

Fig. A 7 – Plasmid map of pCBFD1, purchased from Addgene with pAC-BETAipi.

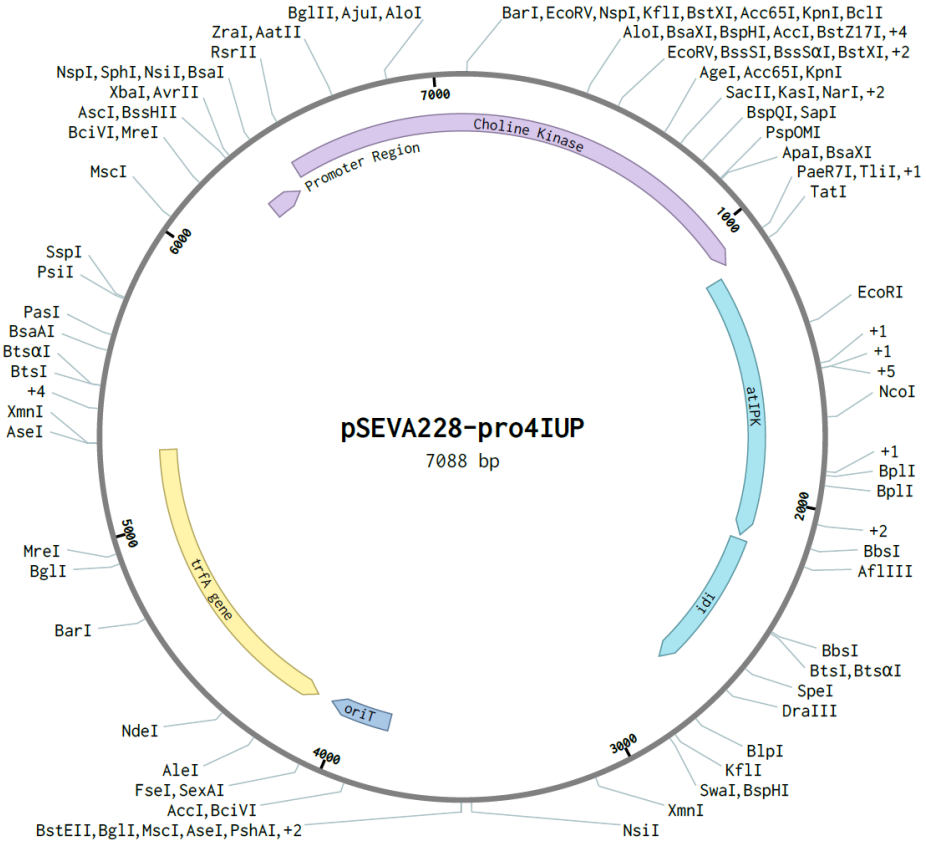

Fig. A 8 – Plasmid map of pSEVA228-pro4IUP, which contains the IUP pathway genes *ck* and *ipk*.

Appendix B: Raw Data

Table B 1 – Strains 1 – 3 in LB media with immediate induction (n=3 ± 1σ).

	Strain 1		**Strain 2**		**Strain 3**	
Growth Time (h)	Cell Density (g/L)	Carotenoid Conc. (mg/L)	Cell Density (g/L)	Carotenoid Conc. (g/L)	Cell Density (g/L)	Carotenoid Conc. (g/L)
0	0.00±0.00	0.00±0.00	0.00±0.00	0.00±0.00	0.00±0.00	0.00±0.00
6	0.50±0.17	0.37±0.03	0.33±0.12	0.50±0.05	0.20±0.17	0.23±0.01
12	1.90±0.17	0.77±0.20	1.20±0.17	2.45±0.17	1.33±0.06	1.13±0.15
24	2.07±0.38	2.25±0.33	1.27±0.15	5.75±0.47	1.33±0.21	2.89±0.48
36	1.73±0.21	1.91±0.25	1.33±0.15	6.27±0.66	1.33±0.15	3.45±0.44
48	2.13±0.15	1.60±0.14	1.47±0.23	6.24±1.01	1.40±0.20	3.37±0.28

Table B 2 – Strains 4 – 6 in LB media with immediate induction (n=3 ± 1σ).

	Strain 4		**Strain 5**		**Strain 6**	
Growth Time (h)	Cell Density (g/L)	Carotenoid Conc. (mg/L)	Cell Density (g/L)	Carotenoid Conc. (g/L)	Cell Density (g/L)	Carotenoid Conc. (g/L)
0	0.00±0.00	0.00±0.00	0.00±0.00	0.00±0.00	0.00±0.00	0.00±0.00
6	0.53±0.06	0.11±0.02	0.27±0.12	0.27±0.02	0.13±0.06	0.12±0.02
12	1.00±0.20	0.58±0.08	0.83±0.21	0.38±0.03	0.33±0.06	0.19±0.01
24	4.67±0.12	1.23±0.16	1.57±0.06	4.99±0.36	1.03±0.23	2.08±0.24
36	1.83±0.15	0.94±0.12	1.67±0.15	6.25±0.58	1.17±0.21	2.28±0.18
48	1.77±0.06	0.76±0.09	1.63±0.32	5.82±0.96	1.20±0.26	2.12±0.26

Table B 3 – Strains 1 – 3 in LB media when induced at an OD_{600} of 0.5 (n=3 ± 1σ).

	Strain 1		**Strain 2**		**Strain 3**	
Growth Time (h)	Cell Density (g/L)	Carotenoid Conc. (mg/L)	Cell Density (g/L)	Carotenoid Conc. (g/L)	Cell Density (g/L)	Carotenoid Conc. (g/L)
0	0.53±0.06	0.12±0.03	0.57±0.06	0.29±0.02	0.50±0.17	0.24±0.04
6	1.20±0.20	0.73±0.05	1.07±0.12	1.74±0.15	0.87±0.06	1.03±0.08
12	1.80±0.30	1.78±0.14	1.40±0.40	4.30±0.44	1.10±0.17	1.87±0.16
24	2.17±0.29	2.28±0.25	1.83±0.29	5.43±0.44	1.57±0.21	4.16±1.86
36	2.47±0.47	2.11±0.27	2.13±0.25	6.05±0.95	1.37±0.29	3.81±0.13
48	2.67±0.58	2.43±0.86	2.17±0.21	5.85±0.94	1.37±0.25	3.57±0.22

Table B 4 – Strains 4 – 6 in LB media when induced at an OD_{600} of 0.5 (n=3 ± 1σ).

	Strain 4		**Strain 5**		**Strain 6**	
Growth Time (h)	Cell Density (g/L)	Carotenoid Conc. (mg/L)	Cell Density (g/L)	Carotenoid Conc. (g/L)	Cell Density (g/L)	Carotenoid Conc. (g/L)
0	0.17±0.06	0.04±0.03	0.23±0.06	0.28±0.03	0.23±0.06	0.13±0.03
6	0.73±0.15	0.12±0.01	0.60±0.10	0.83±0.18	0.43±0.06	0.30±0.01
12	1.23±0.25	0.49±0.09	1.27±0.21	1.09±0.16	0.90±0.10	0.44±0.11
24	1.23±0.06	0.81±0.16	1.53±0.12	4.82±0.74	1.47±0.15	2.16±0.30
36	1.90±0.17	0.60±0.13	1.73±0.21	5.26±0.49	1.43±0.06	2.27±0.27
48	1.63±0.15	0.53±0.09	1.43±0.16	6.00±0.47	1.37±0.15	2.00±0.29

Table B 5 – Strains 1 – 3 in M9 media when induced at an OD_{600} of 0.5 (n=3 ± 1σ).

	Strain 1		**Strain 2**		**Strain 3**	
Growth Time (h)	Cell Density (g/L)	Carotenoid Conc. (mg/L)	Cell Density (g/L)	Carotenoid Conc. (g/L)	Cell Density (g/L)	Carotenoid Conc. (g/L)
0	0.47±0.06	0.34±0.02	0.57±0.06	0.84±0.03	0.73±0.15	0.55±0.05
6	0.83±0.21	0.86±0.03	0.70±0.17	0.95±0.08	0.97±0.21	2.15±0.11
12	0.97±0.21	0.83±0.06	0.73±0.12	1.04±0.07	1.20±0.36	4.39±0.24
24	1.20±0.52	0.83±0.05	0.87±0.23	1.00±0.11	1.27±0.06	7.49±1.29
36	1.27±0.25	0.85±0.05	0.97±0.15	1.01±0.10	1.17±0.06	9.33±0.94
48	1.23±0.25	0.87±0.05	1.13±0.12	1.03±0.08	1.23±0.21	11.32±0.50

Table B 6 – Strains 4 – 6 in M9 media when induced at an OD_{600} of 0.5 (n=3 ± 1σ).

	Strain 4		**Strain 5**		**Strain 6**	
Growth Time (h)	Cell Density (g/L)	Carotenoid Conc. (mg/L)	Cell Density (g/L)	Carotenoid Conc. (g/L)	Cell Density (g/L)	Carotenoid Conc. (g/L)
0	0.93±0.23	0.14±0.02	0.83±0.15	0.48±0.02	0.27±0.06	0.03±0.02
6	0.87±0.25	0.34±0.05	1.03±0.06	1.15±0.19	0.50±0.10	1.29±0.11
12	0.90±0.36	0.34±0.06	0.87±0.06	1.23±0.07	0.90±0.00	2.41±0.27
24	0.90±0.00	0.30±0.06	0.73±0.12	1.05±0.06	1.07±0.21	3.42±0.40
36	0.90±0.17	0.27±0.04	0.70±0.10	0.99±0.05	1.13±0.15	3.98±0.46
48	0.87±0.12	0.25±0.04	0.73±0.06	0.86±0.01	0.93±0.06	3.12±0.22

Table B 7 – Strains 7 – 9 in M9 media when induced at an OD_{600} of 0.5 (n=3 ± 1σ).

	Strain 7		**Strain 8**		**Strain 9**	
Growth Time (h)	Cell Density (g/L)	Carotenoid Conc. (mg/L)	Cell Density (g/L)	Carotenoid Conc. (g/L)	Cell Density (g/L)	Carotenoid Conc. (g/L)
0	0.27±0.06	0.08±0.03	0.17±0.06	0.06±0.00	0.23±0.12	0.03±0.02
6	0.53±0.06	0.90±0.09	0.47±0.06	1.21±0.18	0.43±0.06	1.12±0.08
12	0.90±0.00	1.16±0.15	0.83±0.06	2.36±0.19	0.90±0.10	2.76±0.20
24	1.03±0.15	1.16±0.16	0.87±0.06	2.49±0.33	1.03±0.06	3.65±0.39
36	1.07±0.12	1.19±0.06	1.20±0.10	2.27±0.14	1.07±0.06	3.28±0.34
48	1.13±0.15	1.19±0.01	1.07±0.12	2.41±0.11	0.90±0.10	2.31±0.23

Table B 8 – Strain 6 in M9 media when induced with 0 – 0.4 mM IPTG (n=3 ± 1σ).

	0.0 mM		**0.2 mM**		**0.4 mM**	
Growth Time (h)	Cell Density (g/L)	Carotenoid Conc. (mg/L)	Cell Density (g/L)	Carotenoid Conc. (g/L)	Cell Density (g/L)	Carotenoid Conc. (g/L)
0	0.13±0.06	0.02±0.01	0.10±0.00	0.03±0.01	0.13±0.06	0.02±0.02
6	0.17±0.06	0.10±0.01	0.13±0.06	0.14±0.03	0.13±0.06	0.17±0.04
12	0.37±0.06	0.98±0.03	0.30±0.00	0.38±0.02	0.20±0.00	0.36±0.03
24	0.60±0.10	3.27±0.27	0.30±0.10	0.57±0.03	0.33±0.06	0.48±0.05
36	0.87±0.06	3.83±0.34	0.47±0.06	0.88±0.03	0.57±0.15	1.06±0.21
48	1.10±0.17	5.01±0.81	0.50±0.00	2.36±0.11	0.77±0.32	4.39±1.85
60	1.10±0.10	5.11±0.90	0.77±0.06	3.35±0.45	0.93±0.15	5.67±2.09
72	1.10±0.01	5.86±0.96	1.20±0.35	4.07±0.48	1.43±0.21	5.94±1.88

Table B 9 – Strain 6 in M9 media when induced with 0.5 – 1 mM IPTG (n=3 ± 1σ).

	0.5 mM		0.7 mM		1.0 mM	
Growth Time (h)	Cell Density (g/L)	Carotenoid Conc. (mg/L)	Cell Density (g/L)	Carotenoid Conc. (g/L)	Cell Density (g/L)	Carotenoid Conc. (g/L)
0	0.10±0.00	0.00±0.01	0.10±0.00	0.01±0.02	0.10±0.00	0.01±0.01
6	0.30±0.10	0.15±0.02	0.27±0.06	0.14±0.02	0.23±0.06	0.16±0.04
12	0.53±0.23	0.30±0.05	0.47±0.15	0.40±0.09	0.47±0.15	0.32±0.04
24	0.57±0.06	0.49±0.13	0.50±0.00	0.54±0.03	0.53±0.06	0.50±0.08
36	0.70±0.17	1.44±0.15	0.67±0.06	1.31±0.17	0.60±0.10	1.27±0.21
48	0.93±0.06	4.63±0.78	0.93±0.12	4.41±0.26	0.87±0.15	4.54±0.32
60	1.03±0.15	6.31±0.49	0.93±0.12	6.01±0.88	0.93±0.06	6.06±1.15
72	1.03±0.06	7.64±0.30	0.83±0.06	7.79±1.20	0.87±0.06	7.92±0.99

Table B 10 – Strain 6 in M9 media when casamino acids are added to the media (n=3 ± 1σ).

Strain 6 + 5 g/L Casamino Acid		
Growth Time (h)	Cell Density (g/L)	Carotenoid Conc. (mg/L)
0	0.23±0.06	0.05±0.01
1	0.37±0.06	0.09±0.01
2	0.43±0.12	0.25±0.03
3	0.50±0.00	0.55±0.05
6	0.53±0.06	1.51±0.15
12	0.77±0.12	2.32±0.28
24	0.87±0.12	3.11±0.35
36	1.07±0.06	3.26±0.35
48	1.23±0.06	4.62±0.89

Table B 11 – MG1655 *E. coli* with p5T7-lycipi-ggpps and the IUP pathway at two different temperatures (n=3 ± 1σ).

	30°C		**37°C**	
Growth Time (h)	Cell Density (g/L)	Carotenoid Conc. (mg/L)	Cell Density (g/L)	Carotenoid Conc. (g/L)
0	0.13±0.06	0.02±0.01	0.20±0.00	0.01±0.01
6	0.33±0.12	0.07±0.07	0.53±0.06	0.14±0.03
12	0.50±0.00	0.11±0.02	0.67±0.06	0.27±0.03
24	0.60±0.10	0.26±0.04	0.97±0.06	1.07±0.13
36	0.70±0.10	1.20±0.25	1.27±0.12	4.71±0.43
48	0.77±0.06	4.71±0.59	1.60±0.10	11.25±0.53

Appendix C: Carotenoid Standard Curves and HPLC Results

Table C 1 – Absorbance data of pure carotenoids for the preparation of calibration curves (n=2 ± 1σ).

Concentration (mg/L)	Astaxanthin (abs)	β-Carotene (abs)	Lycopene (abs)
0.0	0.000±0.001	0.000±0.000	0.000±0.001
0.1	0.017±0.009	0.005±0.002	0.017±0.000
0.2	0.019±0.001	0.012±0.000	0.024±0.006
0.3	0.026±0.001	0.018±0.001	0.023±0.005
0.4	0.036±0.005	0.025±0.001	0.028±0.007
0.5	0.045±0.001	0.036±0.004	0.046±0.009
1.0	0.076±0.008	0.063±0.008	0.087±0.008
2.0	0.161±0.001	0.132±0.006	0.160±0.004
3.0	0.240±0.014	0.200±0.005	0.239±0.009
4.0	0.308±0.016	0.270±0.007	0.344±0.035
5.0	0.365±0.013	0.352±0.011	0.430±0.002
10.0	0.821±0.076	0.664±0.065	0.801±0.001

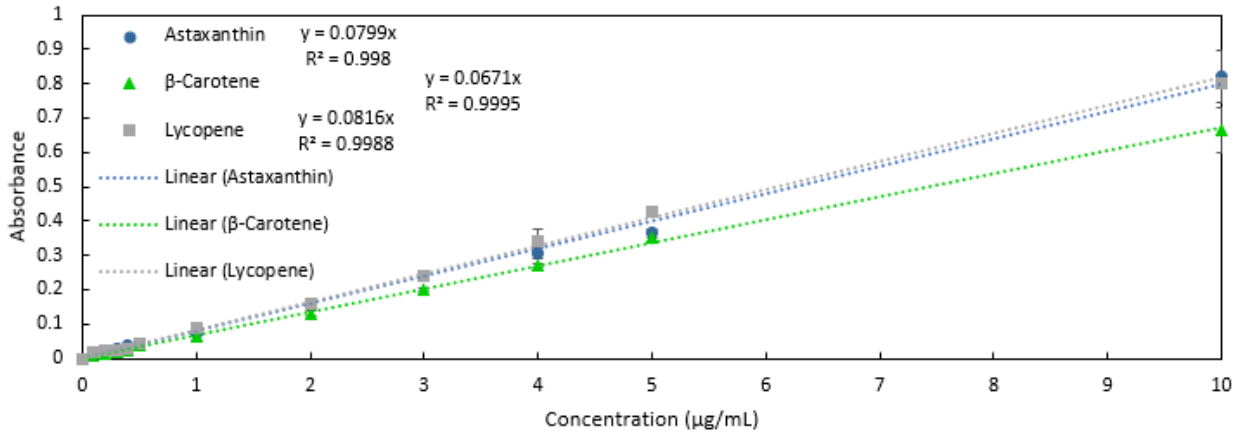

Fig. C 1 – Standard curves for astaxanthin, lycopene and β-carotene at 475 nm using the 96-well plate reader. The astaxanthin standard curve was used in all experiments, except for analyzing the performance of p5T7-lycipi-ggpps, which used the lycopene standard curve.

Table C 2 – Calibration curves with respect to chromatogram peak area using HPLC for the five carotenoid standards.

Astaxanthin		**Canthaxanthin**		**Zeaxanthin**		**Lycopene**		**β-Carotene**	
Conc. (mg/L)	**Area**	**Conc. (mg/L)**	**Area**	**Conc. (mg/L)**	**Area**	**Conc. (mg/L)**	**Area**	**Conc. (mg/L)**	**Area**
0	0.0	0	0.0	0	0.0	0	0.0	0	0.0
3	321.6	1	70.3	3	271.0	1	102.4	1	85.7
6	586.8	2	77.0	6	553.5	2	173.9	2	170.0
9	890.0	3	116.2	9	888.9	3	250.1	3	258.9
12	1158.6	4	163.8	12	1206.3	4	316.7	4	339.5
15	1500.9	5	204.5	15	1491.2	5	402.6	5	394.6
Slope	98.8108	40.9099		98.9464		81.4592		82.4290	
R-Sq.	0.9989	0.9712		0.9989		0.9963		0.9957	
Retention Time (min)	2.71	3.23		2.71		13.67		3.99	

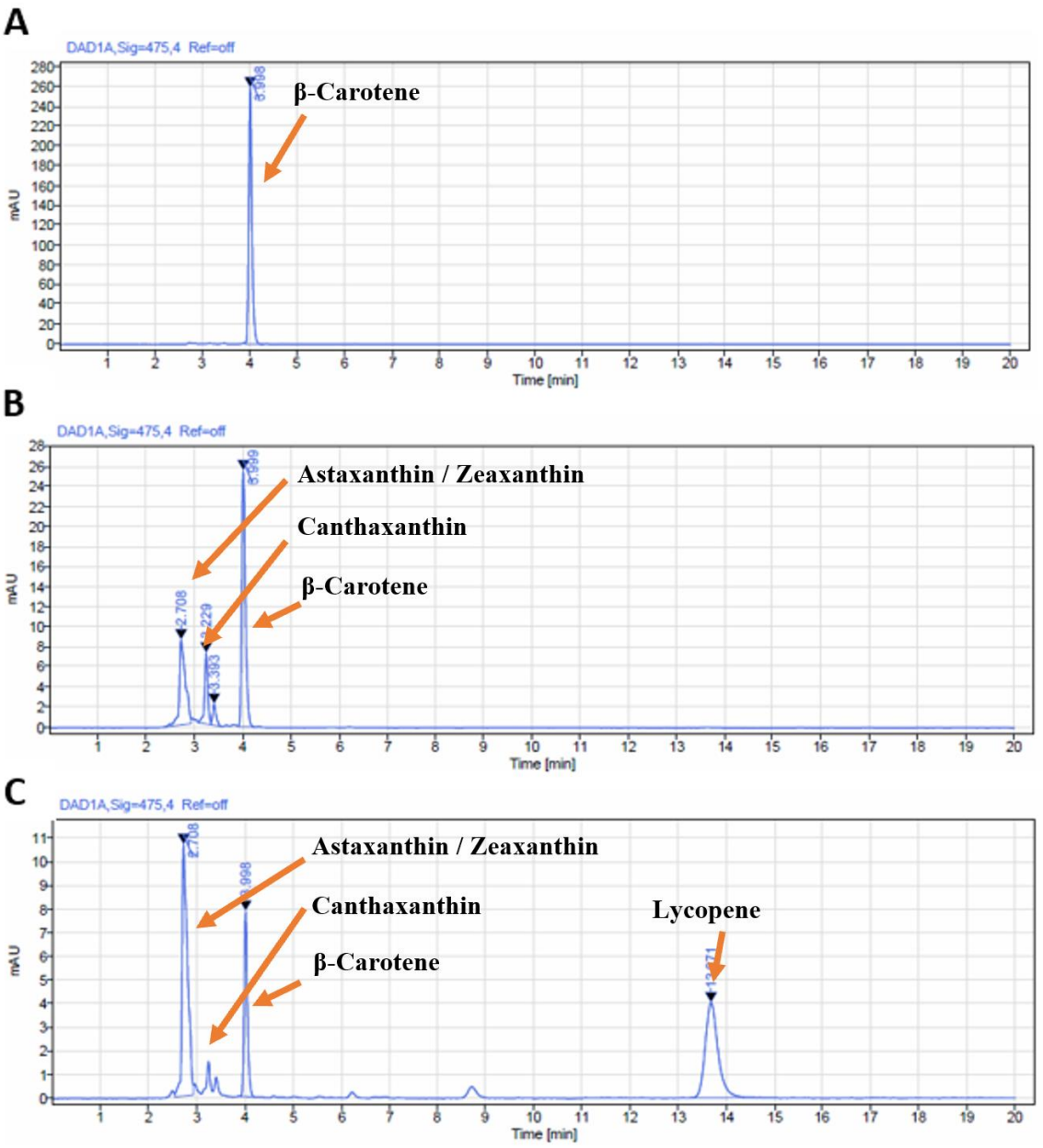

Fig. C 2 – Representative chromatograms for the carotenoid-producing IUP strains. The identities of the known peaks are indicated. These were run in triplicate. **A:** Strain 3. **B:** Strain 6. **C:** Strain 9.

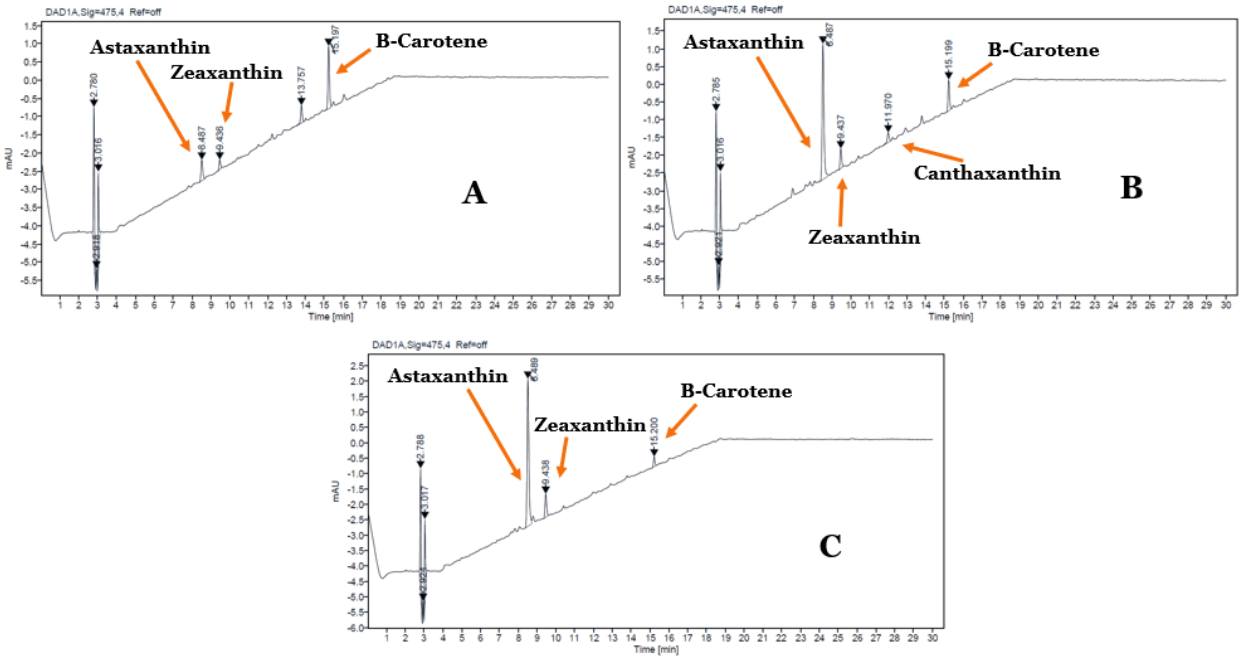

Fig. C 3 – Sample chromatograms from the revised HPLC experiment. The identities of the known peaks are indicated. These were run in triplicate. **A:** Strain 3. **B:** Strain 6. **C:** Strain 9.